**EUROPEAN UNION**
EUROPEAN FUND FOR MARITIME AFFAIRS AND FISHERIES

MINISTRY OF AGRICULTURE

MARITIME AFFAIRS AND FISHERIES PROGRAM

# MULTISPECIES TRAWL SURVEY IN THE BULGARIAN WATERS OF THE BLACK SEA,

# November 2022

## SCIENTIFIC REPORT

**Violin Raykov et al, 2022**

www.eufunds.bg

*Проект № BG14MFOP001-3.003-0004, „Събиране, управление и използване на данни за целите на научния анализ и изпълнението на Общата политика в областта на рибарството за 2022 г.“, финансиран от Програмата за морско дело и рибарство, съфинансирана от Европейския съюз чрез Европейския фонд за морско дело и рибарство.*

**EUROPEAN UNION**
EUROPEAN FUND FOR MARITIME AFFAIRS AND FISHERIES

MINISTRY OF AGRICULTURE

MARITIME AFFAIRS AND FISHERIES PROGRAM

This study was carried out thanks to the financial support of the European Commission under REGULATION (EU) 2017/1004 OF THE EUROPEAN PARLIAMENT AND OF THE COUNCIL of 17 May 2017 on the establishment of a Union framework for the collection, management and use of data in the fisheries sector and support for scientific advice regarding the common fisheries policy and repealing Council Regulation (EC) No 199/2008 (recast), the National Agency for Fisheries and Aquaculture – Ministry of Agriculture, Bulgaria and Institute of Oceanology – BAS, Varna, Bulgaria.

Project № BG14MFOP001-3.003-0004, "Collection, management and use of data for the purpose of scientific analysis and implementation of the Common Fisheries Policy for 2022", funded by the Maritime and Fisheries Program and co-financed by the European Union through the European Maritime and Fisheries Fund.

The survey was carried out in November 2022 in the Bulgarian Black Sea area on board of R/V *HAITHABU* in execution of the National Program of Bulgaria for data collection.

BULGARIAN ACADEMY OF SCIENCES

INSTITUTE OF OCEANOLOGY

VARNA

Assoc. Prof. Violin Raykov, Assoc. Prof. Maria Yankova, Assoc. Prof. Petya Ivanova, Assoc. Prof. Veselina Mihneva, Assoc. Prof. Dimitar Dimitrov, Assoc. Prof. Kremena Stefanova, Chief Asst. Elitsa Stefanova,Ilian Kotsev, Chief Asst. Nina Dzhembekova, Chief Asst.Ivelina Zlateva, Nelly Valcheva (technician), Dobroslav Dechev (technician), Hristiyana Stamatova (technician), Svetla Koleva (technician), Petar Trandafilov (logistics).

## Table of content





*Project № BG14MFOP001-3.003-0004 Collection, management and use of data for the purpose of scientific analysis and implementation of the Common Fisheries Policy for the period 2022, funded by the Maritime and Fisheries Program and co-financed by the European Union through the European Maritime and Fisheries Fund*

# 1. Introduction

Pelagic Trawl Surveys were accomplished in November 2022 in the Bulgarian Black Sea zone. A scientific team has produced a biological analysis of the results obtained from the survey. The biological analysis is based on the biomass of the species found during the study. Besides, an analysis of the distribution and abstraction of the other species caught as by-catch is presented. Sprat (*Sprattus sprattus*) is a key species for the Black Sea ecosystem. Together with the anchovy, sprat is one of the most abundant, planktivorous, pelagic species. The level of its stocks depends on the conditions of the environment mainly and on the fishing effort.

The changes in the environment due to anthropogenic impact affect the dry land as well as the world ocean. The level of sea pollution and its "self-purifying" ability is completely different. There is a clear indication of changes in the natural equilibrium in the corresponding ecological niches (Prodanov et al., 1997). The greatest impact on the world ocean is commercial fishery, which directly devastates a significant part of the given species populations.

As a result of this, some of the species' stocks have declined or depleted. As a result of the excessive exploitation, altered habitats and climatic variations numerous of the commercial species are critically endangered or vulnerable. The abundance of the given fish species generations is dependent on different abiotic and biotic factors. With great importance is the level of fishing mortality, changes in trophic levels due to mass occurrence of the ctenophore *Mnemiopsis leidyi*, algal blooms which lead to hypoxia in the shallower waters with mass mortality of the bottom-dwelling organisms, etc.

The recent state of the sprat stock biomass (aggregations) off the Bulgarian Black sea coast show relative stability, i.e. taking into consideration the almost constant level of exploitation (in the western and north-western part of the Black Sea) in recent years, the stock has not yet been sufficiently exploited.

Estimates of the number and size distributions of fish stocks based on experimental trawling have become a necessity in fisheries management (GodØ et al., 1990). The main assumption in these studies is that the level of catches is constant, no matter how long the trawling is. Any deviation from the linear dependence between the catch and the magnitude of the effort applied to the fishery can have a significant impact on the composition of the catches and the estimates of the numbers and deviate from the results of the trawl studies (Wassenberg et al., 1998). The duration of the fishing effort during the trawling period may last up to 200 min (GodØ et al., 1990), but for economic reasons, together with the need for multiple reps and maintaining statistical validity, the duration of trawling is reduced. Thus, the standard trawl duration varies from 30 to 120 minutes for each selected station. Some authors (Godø et al., 1990; Somerton et al., 2002; Wassenberg et al., 2002) allow larger specimens to swim in the trawl without entering the bag and that trawls of varying lengths may affect the levels of the catches and the size distribution of the trawl. In this way, some size groups may not be captured in short-haul trawls.

The average catch per unit of effort or unit area is the inventory of the stock (assumed to be proportional to the stock). These indices can be converted into an absolute measure for biomass by the so-called "area method" which is also referred to as a holistic method (www.fao.org).

The theoretical justification of the method is given by Gulland (1975), Saville (1977), Troadec (1980), Doubleday (1980) and Grosslein and Laurec (1982). Planning, design, data collection, data recording, analysis and reporting are summarized in Butler et al. (1986), ICOD (1991) and Strømme (1992).

The "area method" extrapolates the average catch by the research vessel per unit net area trawled to the entire study area (Saville, 1977). This method assumes a random distribution of fish in a given area and 100% gear efficiency in catching all fish. But in practice, catchability is not 100% in all cases (Kock, 1992). Thus the biomass estimate can be underestimated if there is a lack of balancing of the trawl boards, stops and weights, i.e. the so-called a "drive-through" effect to the trawl inlet (Kock, 1985).

The pelagic trawl survey (OTM) was accomplished on the board of research vessel *HaitHabu* (Pic. 1).


**Picture 1.** R/V HaitHabu

**The main characteristics of the ship:**

IMO: 8862686

MMSI: 207139000

Call sign: LZHC
Flag: Bulgaria [BG]
AIS Vessel Type: Other
Gross Tonnage: 142
Length Overall x Breadth Extreme: 24.53m × 8m
Crew: 6
The size of the pelagic trawl are as follows:

- Pelagic trawl type 50/35 – 74 m
- Headroap length – 40 m
- Horizontal opening – 16 m
- Vertical opening – 7 m
- Mesh size – 7x7 mm
- Effective part of trawl – 27 m
- Pelagic doors – 3.5 $m^2$

The trawling was performed during the day with a duration of 30 - 40 minutes, depending on the hydro-meteorological conditions at an average speed of 2.7 knots (variation in the range 2.7-2.9).

## 2. Materials and Methods

Pelagic Trawl surveys were accomplished following National Programs for Data Collection in the Fisheries sector of Bulgaria for 2022. The study was conducted in November 2022, in the area enclosed between Durankulak and Ahtopol (Bulgaria) with a total length of the coastline of 370 km. The study area encloses waters between 42º05’ and 43º45’ N and 27º55 and 29º55 E.
During the survey, a total of 37 mid-water hauls were carried out in the Bulgarian area (July 2022). The survey took place during the day and the following types of data were collected:

- Coordinates and duration of each trawl
- Sprat total catchweight
- Separation of the by-catch by species
- Composition of by-catch
- Conservation of the samples

## 2.1. Sampling design

To establish the abundance of the reference species (*Sprattus sprattus*) in front of the Bulgarian coast a standard methodology for stratified sampling was employed (Gulland, 1966). To address the research objectives the region was divided into 3 strata according to depth: Stratum 1 (15 - 30 m), Stratum 2 (30 – 50 m) and Stratum 3 (50 – 100m).

The study area in Bulgarian waters was partitioned into 128 equal in size, not overlapping fields, situated at a depth between 15 - 100 m. At 37 of the fields chosen at random, sampling employing midwater trawling was carried out (Pic. 2.1.1).

**Picture 2.1.1.** Trawling operation with R/V Hait Habu

Each field was a rectangle with sides 5' Lat × 5' Long and area around 62.58 $km^2$ (measured by application of GIS), large enough for a standard lug extent in meridian direction to fit within the field boundaries. The fields were grouped in larger sectors, so-called strata, in which geographic and depth boundaries were selected according to the density distribution of the species under study. At each of the fields, only one haul with duration between 30 - 40 min at speed 2.7-2.9 knots was carried out (Pic. 2.1.2).

**Picture 2.1.2.** Catch in trawl with R/V HaitHabu

## 2.2. Onboard sample processing

The number of processed individuals is presented in Table 2.2.1.

**Table 2.2.1.** Number of processed individuals

| Species | Number |
|---|---|
| Sprat | 59 |
| Whiting | 1000 |
| Red mullet | 1000 |
| Horse mackerel | 1000 |
| Anchovy | - |

**Picture 2.2.1.** Catch and by-catch in OTM

The data recorded and samples collected at each haul include (Gulland,1966):

- Depth, measured by the vessel's echo sounder
- GPS coordinates of start/end haul points
- Haul duration
- An abundance of sprat caught
- Weight of total sprat catch
- Abundance and weight of other large species
- Species composition of by-catch

4% Formaldehyde solution with marine water was used for the conservation of sprat for stomach content examination.

## 2.3. Laboratory analyses

The samples collected onboard were processed in a laboratory for determination of age and food composition.
The age was established in otoliths under the binocular microscope.
The food spectrum was determined by separation of the stomach contents into taxonomic groups identified to the lowest possible level.

## 2.4. Statistical analyses

*Swept area method*

This method is based on bottom trawling across the seafloor (area swept), weighted with chains, rock-hopper, and roller gear, or steel beams. Widely used a direct method for demersal species stock assessment (Fig. 2.4.1., 2.4.2.).

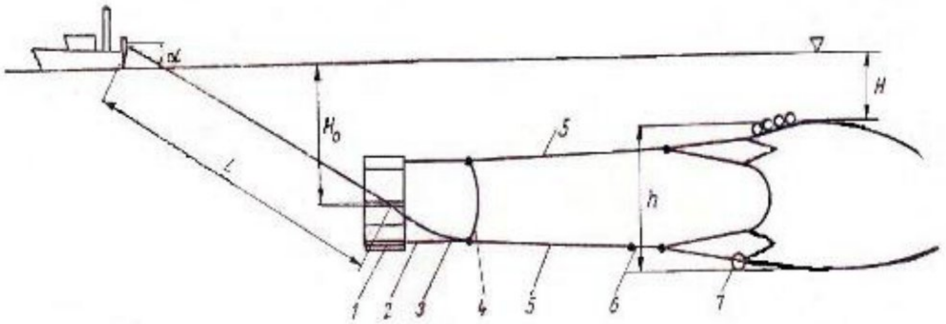


**Figure 2.4.1.** Scheme of the trawl, used in the Swept area method (according to Grudev et al., 1981) 1 - trawl door; 2 - conjections; 3 - transitional wire; 4 - compensator; 5 - wires; 6 - extention cord; 7- deepener.

On Figure 2.4.2. is represented the scheme of bathy-pelagic trawl for sprat catch.

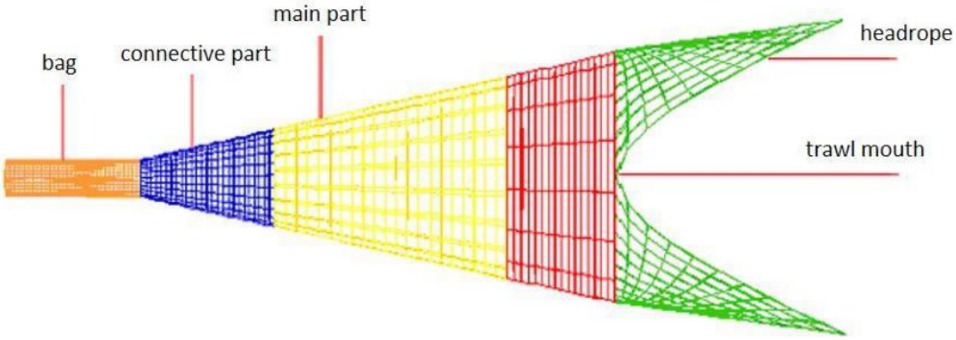


**Figure 2.4.2.** Scheme of bathy-pelagic trawl for sprat catch

The main point of the method: the trawl doors are designed to drag along the seafloor for defined distance. Trawling area was calculated as follows:

$$a = D * hr * X2$$

(1) $D = V * t$

(Where: a – trawling area, V – trawling velocity, hr* X2 – trawl door distance, t – trawling duration (h), D – dragged distance on the seafloor;

(2) $D = 60 * \sqrt{(Lat_1 - Lat_2)^2 + (Lon_2 - Lon_1) * \cos(0.5 * (Lat_1 + Lat_2))}$

(3) $D = \sqrt{VS^2 + CS^2 + 2 * VS * CS * \cos(dirV - dirC)}$,

Where, $VS$ is vessel velocity, $CS$ - present velocity (knots), dir$V$ vessel course (degrees), and $dirC$- present course (degrees).

Stock biomass is calculated using catch per unit area, as a fraction of catch per unit effort from the dragged area:

(4) $(\frac{C_{w/t}}{a/t}) = C_{w/a} kg / sq.km$

Where: *Cw/t* – catch per unit effort, a/t – trawling area (km$^2$) per unit time;

Stock biomass of the given species per each stratum could be calculated as follows:

(5) $$B = (\overline{C_{w/a}}) * A$$

Where: $\overline{C_{w/a}}$ - mean CPUA for total trawling number in each stratum, A- area of the stratum.

The variance of biomass estimate for each stratum is (equation 4):

(6) $$VAR(B) = A^2 * \frac{1}{n} * \frac{1}{n-1} * \sum_{i=1}^{n} \left[Ca(i) - \overline{Ca}\right]^2$$

The total area of the investigated region is equal to the sum of areas of each stratum:

$A = A1+A2+A3$

Average weighted catch per whole aquatic territory is calculated as follows:

(7) $$\overline{Ca}(A) = Ca1 * A1 + Ca2 * A2 + Ca3 * A3 / A$$

Where: Ca1- catch per unit area in stratum 1, A1 – an area of stratum 1, etc., A- size of total area. Accordingly, total stock biomass for the whole marine area:

(8) $$B = \overline{Ca}(A) * A$$

Where: $\overline{Ca}(A)$- average weighted catch per whole investigated marine area, A – total investigated marine area.

*Estimation of Maximum Sustainable Yield (MSY)*

The Gulland's formula for virgin stocks is used (equation 7):
(9) MSY = 0.5*M*Bv

where: M – coefficient of natural mortality; Bv – virgin stock biomass.

*A relative yield-per-recruit model with uncertainties*

$$Y'/R = E * U^{M/k} \left\{ 1 - \frac{3U}{(1+m)} + \frac{3U^2}{(1+2m)} - \frac{U^3}{(1+3m)} \right\}$$ (10)

where: $U = 1-(Lc/L\infty)$

$m = (1-E)/(M/k) = k/Z$

$E = F/Z$ – exploitation coefficient.

*Lenght-converted catch curve*

Several methods are available with the help of which total mortality (Z) can be estimated from length-frequency data. Thus, it is possible to obtain reasonable estimates of Z from the mean length in a representative sample or the slope of Jones' cumulative plot. In this article, a variety of approaches for analyzing length-frequency data are presented which represent the functional equivalent of [age structured] catch curves. These "length-converted catch curves" are built around assumptions similar to those involved in age-structured catch curves.

### 2.5. Age estimation

As it is well known, the Calcified Structures (CS) are usually used to assign age useful to obtain their growth model and so, to reconstruct age composition of exploited fish populations. Fish aging implies the presence in the CS of a structural pattern, in terms of succession of opaque and translucent zones and the knowledge of the periodicity of this deposition pattern. Calcified structures available for fish aging are different: otoliths (sagittal, lapilli, asterischi), scales, vertebrae, spines, and opercular bones (Panfili et al., 2002). For the selected stocks the CS utilized is the sagittae. The most important aspects (difficulties, extraction, storage, preparation method, aging criteria) regarding the age analysis are addressed by species.
Otoliths are important for fish and fisheries scientists. Otoliths are playing role of balance, motion, and sound. These structures are effective from growth to death in the entire life cycle. They are most commonly used to determine growth age and for mortality studies. Research on otoliths began in the 1970s and continued to 21st century. Periodic growth increments in scales, vertebrae, fin rays, in cleithra, opercula, and otolith are used to determine annual age in many fish species. Researchers used otolith reference collections and photographs in publications to aid in identification (Pic. 2.5.1). Otoliths have a distinctive shape that is highly specific but varies widely among species.

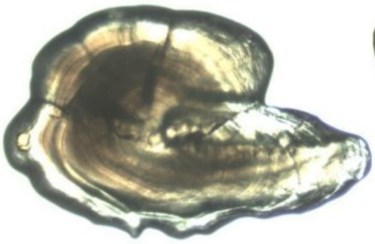

6 cm (0+)

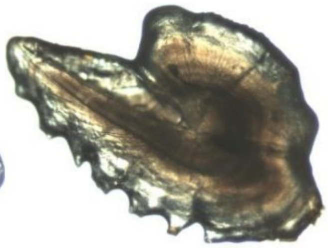

7.5 cm (1+)

8.2 cm (1+)

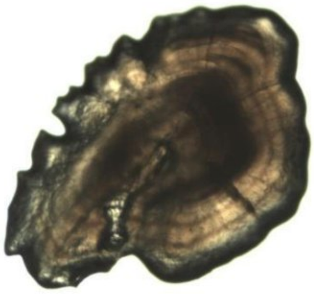

9 cm (2+)

9.5 (3+)

10.7 (4+)

**Picture 2.5.1.** Otoliths of sprat

Biologists, taxonomists, and archaeologists, based on the shape and size of otoliths determine fish predators feeding habits (Kasapoglu and Duzgunes, 2014). In teleost fishes, otoliths are the main CS for age determination and it is widely used in fisheries biology. On the other hand, analyzing $O_2$ isotopes in their structure is useful to determine fish migrations between freshwater and sea as well as species and stock identification. Otoliths are the balance and hearing organs for the fish. They are three types located on the left and right side of the head in semi rings: “sagitta” in the saccular, “lapillus” in the lagenar, and “asteriskus” in the utricular channels. Place, size, and shape of these three types are different by species, the biggest one is sagitta and the smallest one is asteriscus. So, sagitta is the one mostly used in age determination in bony fishes. Other reasons for the preference to otoliths are:

- Their formation in the embryonic phase which shows all the changes in the life cycle of the fish.
- Existence in the fish which have no scales.
- Giving better results than the scales and more successful age readings in older fish than their scales.
- No restoration or regeneration.
- Having the same structure in all the individuals in the same species (Jearld, 1983).

On the other hand, their disadvantages are the obligation of dissecting the fish and some failures in age determination due to crystal-like formations by irregular $CaCO_3$ accumulations on the otoliths.

### 2.5.1. Preparation for otolith extraction

For the sampling of fish for otolith extraction from the overall samples is very important to have representative samples for the catch. The number of otoliths needed is lower for the species having a smaller size range than the species having a larger size range. According to the availability, 5 fish for each length group may be better for age readings to be representative of the population.For each fish total length (±0,1 cm), total weight (±0,01g), sex, maturation stage (I-V), gonad weight (±0,01g) are recorded.

Sagittal otoliths of each fish are removed by cutting the head over the eyes after all individual measurements. Then, rinsed and immersed in 96% ethyl alcohol to get rid of organic wastes/residuals and finally kept in small chambers in plastic roomed boxes with the sample number and other operational information.

### 2.5.2. Preparation of the otoliths for the age determination

Otoliths are put into small black convex glasses containing 96% ethyl alcohol for age readings under the binocular stereo microscope which is illuminated from top and sides (Fig. 2.5.2.1) (Polat and Beamish, 1992). The magnifying level depends on the size of the otolith; X4 is good for sprat and X1 for turbot.

**Figure 2.5.2.1.** Binocular stereo microscope with top and side illumination

### 2.5.3. Age readings and commenting on annuluses

To prevent bias, during age reading readers should not refer to the length and weight of that fish. But information on the date of the catch and gonadal state is very important. The first step is to clarify the place of the center and the first age ring. After that, observation of the successive rings, whether they are continuous or not, is important.

Finally, determination of the fish in growth or just at the end of the growth period by checking characteristics of the ring at the edge of the otolith to decide if it is opaque or hyaline. After these procedures otoliths can be read under these protocols which are very important to provide data on age to determine realistic population parameters and reduce uncommon procedures and biases by standardized age reading criteria.

For sprat, the left and right otoliths show isometric growth. They are small and transparent (Fig. 2.5.3.1). Age readings can be done over the otolith surface by clear ring views. Due to summer and winter growths, there are two different nucleus formations in the center; spring recruits have opaque, late fall recruits have hyaline rings which are taken into consideration during age readings (Pısıl, 2006).

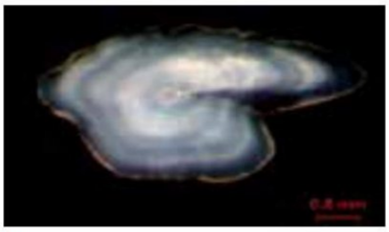

a

b

TL: *a* – 6.2 cm; *b* – 6.7 cm

*S. sprattus*

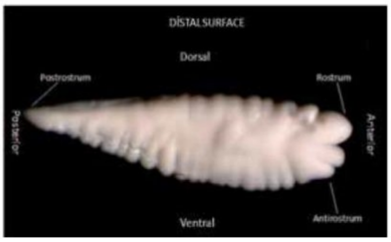


*Merlangius merlangus*

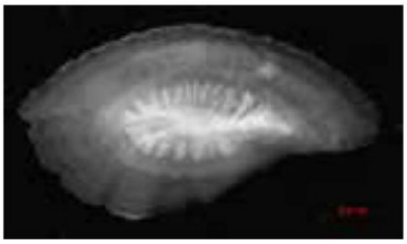

*Trachurus mediterraneus*

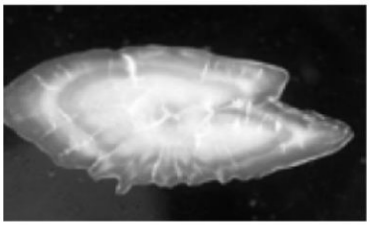

*E. encrasicolus*

*P. salstarix*

*M. barbatus*

**Figure 2.5.3.1.** Sprat, anchovy, horse mackerel, red mullet, bluefish otoliths

### 2.5.4. Age reading protocol for sprat

1. Dissected otoliths rinsed and treated with 96% ethyl alcohol and stored dry.
2. Readings were carried out by inspecting the whole otolith in 96% ethyl alcohol in black colored convex glass bowl under reflected light against a dark background.
3. Magnification was set considering the biggest otolith size which fitted the visual capacity of the lens. It was aimed not to change magnification rate which might enable false rings visible in bigger otoliths and permitted to see true rings (hyalines) better by unchanging the color contrasts. That's why magnification rate X4 was selected for the sprat otoliths.
4. Otolith samples were observed from the distal surface as a whole, broken ones were not used.
5. Birthday of the sprat is accepted as 1st of January as the common principle for the fish living in the Northern hemisphere in line with the subtropical fish growth models.
6. Central point surrounded by the hyaline rings, which is one in some cases or two for the others, is formed after the end of consumption of yolk sac and starting of free feeding, known as “stock rings”. Next opaque accumulation is known as the “first-year growth ring”. This ring keeps its circular form in the postrostrum region. Both, this ring and the next hyaline ring forming “V” shape in the rostrum, are accepted as first age rings.
7. Tiny and continuous concentric rings prolonged close to the real hyaline ringe are counted together with the real one as one age. This ring may be either a very tiny and opaque one inside the hyaline band or a tiny hyaline ring near the outer edge of the opaque ring.
8. Sprat and some other short-lived species have a very fast growth rate, especially in the first two years. Width of the growth bands after the 2nd year ring becomes relatively narrower. This issue should be kept in mind in the older age ring readings.

The number of tiny and weak hyaline rings, known as false rings, in the opaque region, is not so high and their separation from age rings is rather easy. When they are so much and inseparable, these otoliths should not be used.

### 2.6. Sex and maturity estimation

The European sprat (*Sprattus sprattus* L.) is a small short-lived pelagic species from the family Clupeidae. Sprat has a wide distribution including shelf areas of the Northeast Atlantic, the Mediterranean Sea, and the Baltic Sea. Sprat is most abundant in relatively shallow waters and tolerates a wide range of salinities. Spawning is pelagic in coastal or offshore waters and occurs over a prolonged period that may range from early spring to late autumn. Sprat is an important forage fish in the North Sea and Baltic Sea ecosystems. Commercial catches from pelagic fisheries are mainly used for fish meal and fish oil production. Three subspecies of sprat have been defined: *Sprattus sprattus sprattus* L., distributed along the coasts of Norway, the North Sea, Irish Sea, Bay of Biscay, the western coast of the Iberian peninsula down to Morocco; *Sprattus sprattus phalericus*, R. in the northern parts of the Mediterranean and the Black Sea and

*Sprattus sprattus balticus* S. in the Baltic Sea. Knowledge about stock structure, migration of sprat, and mixing of populations among areas is limited. Questions have been raised about the geographic distribution and separation of stocks and their interaction with neighboring stocks (ICES 2011). The apparent overlap, e.g. between North Sea sprat and English Channel sprat seems very strong, whereas the overlap between North Sea sprat and Kattegat sprat is not as strong and varies between years. A distribution wide phylogeographic study showed that sprat in the western Mediterranean is a subgroup of the Atlantic group and that these two populations are closer to each other than to sprat in the eastern Mediterranean and Black Sea (Debes et al., 2008).

### 2.6.1. Maturity stages

It is very important to use standardized maturity scales for sprat (and all species) to evaluate sampling strategies and timing for accurate classification of maturity to provide reliable maturity determination for both sexes. For sprat, small gonad size and the batch spawnings by several cohorts of eggs over a long period are the main challenges for standardizing a maturity scale.
According to the ICES (2011), present standardized maturity scales of sprat include 6-stages for both sexes (Fig. 2.6.1.1, Table 2.6.1.1).

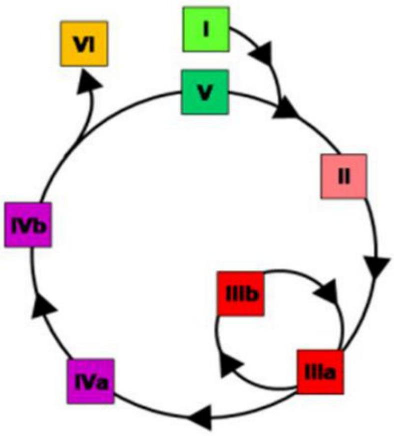


**Figure 2.6.1.1.** Scale with six maturity stages in sprat (Name of the stages are given in Table 2.6.1.1)

In particular, specimens without visible development have been combined into Immature and Preparation, whereas the spawning stage has been sub-divided into a non-active spawning stage (maturing and re-maturing characterized by visible development of gametes) and an active spawning stage indicated by hydrated eggs/running milt. The integration of maturing and re-maturing into the spawning stage allows an accurate determination of maturing and spawning specimens and reliable assessment of the spawning fraction of the population.

**Table 2.6.1.1.** Macroscopic and histological characteristics of gonadal development stages

| *Stages* | *Macroscopic Characteristics* | *Histological characteristics* |
|---|---|---|
| *FEMALES (OG: Oogonia, PG1: Early previtellogenic oocytes, PG2: Late previtellogenic oocytes, CA: Cortil alveoli oocytes, VT1: Early vitellogenic oocytes, VT2: Mid vitellogenic oocytes, VT3: Late vitellogenic oocytes, HYD: Hydrated oocytes, POF: Postovulatory follicles, SSB: Spawning stock biomass).* | | |
| *I-Immature* | *Juvenile: ovaries threadlike and small; transparent to wine red and translucent in color; sex difficult to determine; distinguishable from testes by a more tubular shape; oocytes not visible to the naked eye* | *OG+/-PGI* |
| *II-Preparation* | *The transition from immature to early maturing; oocytes not visible to the naked eye; ovaries yellow-orange to bright red; ovaries occupy up to half of the abdominal cavity. This stage is not included in SSB.* | *PG1, PG2, CA* |
| *III. Spawning* | | |
| *a. Spawning(inactive)* | *Maturing and re-maturing: yolked opaque oocytes visible to the naked eye; ovaries change from semi-transparent to opaque yellow-orange or reddish as more oocytes enter the yolk stage; ovaries occupy at least half of the body cavity; re-maturing ovaries may be red to grey-red or purple in color and less firm than an ovary maturing the first batch, few hydrated oocytes may be left* | *PG1, PG2, CA, VT1, VT2, VT3, +/- POF* |
| *b. Spawning (active)* | *Spawning active. Hydrated eggs are visible among yolked opaque oocytes; hydrates oocytes may be running; ovaries fill the body cavity; overall color varies from yellowish to reddish.* | *PG1, PG2, CA, VT1,VT2, VT3, HYD, POF* |
| *IV.a Cessation* | *Baggy appearance; bloodshot; grey-red translucent in color; atretic oocytes appear as opaque irregular grains; few residual eggs may remain* | *PG1, PG2, POF, atretic oocytes, residual HYD* |

| | | |
|---|---|---|
| *IV.b. Recovery* | *Ovaries appear firmer and membranes thicker than in sub-stage IV.a; these characteristics together with the slightly larger size distinguish this stage from the virgin stage; ovaries appear empty and there are no residual eggs; transparent to wine red translucent in color* | *PG1, PG2, atretic VT oocytes* |
| *V. Resting* | *Ovaries appear more tubular and firmer; oocytes not visible to the naked eye; transparent or grey-white to wine red with well-developed blood supply; this stage leads to stage II.* | *PG1, PG2 +/- atretic oocytes* |
| *VI. Abnormal* | *a) infection; b) intersex - both female and male tissues can be recognized; c) one lobe degenerated; d) stone roe (filled with connective tissue); e) other* | *Abnormal tissue* |
| *MALES (SG: Spermatogonia; PS: Primary spermatocytes; SS: Secondary spermatocytes; ST: Spermatids; SZ: Spermatozoa; SSB: Spawning stock biomass)* | | |
| *I. Immature* | *Juvenile: Testes threadlike and small; white-grey to grey-brown; difficult to determine sex, but distinguishable from ovaries by a more lanceolate shape (knife-shaped edge of the distal part of the lobe).* | *SG, PS* |
| *II-Preparation* | *The transition from immature to mature: Testes easily distinguishable from ovaries by lanceolate shape; sperm development not visible;*<br>*reddish grey to creamy translucent in color; testes occupy up to ½ of the abdominal cavity; this stage is not included in SSB.* | *SG, PS, SS, potentially few ST* |
| *III. Spawning*<br>*a. Spawning(inactive)*<br><br><br><br><br><br><br>*c. Spawning (active)* | *Maturing and re-maturing: Testes occupy at least half of the body cavity and grow to almost the length of the body cavity; the empty sperm duct may be visible; color varies from reddish light grey, creamy to white; edges may still be translucent at the beginning of the stage, otherwise opaque; re-maturing testes may be irregularly colored with reddish or brownish blotches and grey at the lower edge with partly whitish remains of sperm*<br>*Spawning active: testes fill the body cavity; Sperm duct filled and distended throughout the entire length; sperm* | *SG, PS, SS, ST, SZ*<br><br><br><br><br><br><br>*SG, PS, SS, ST, SZ* |

| | | |
|---|---|---|
| | *runs freely or will run from the sperm duct, if transected; color varies from light grey to white..* | |
| *IV.a. Cessation*<br><br><br><br>*IV.b. Recovery* | *Baggy appearance (like an empty bag when cut open); bloodshot; grey to reddish-brown translucent in color; residual sperm may be visible in the sperm duct.*<br>*Testes appear firmer and the testes membrane appears thicker than in stage IVa due to contraction of the testes membrane; these characteristics together with the slightly larger size distinguish this stage from the virgin stage; testes appear empty and no residual sperm is visible in the sperm duct; reddish grey to greyish translucent in color.* | *SG, PS, atretic SS, ST and SZ*<br>*SG, PS, potentially SS, atretic SZ* |
| *V. Resting* | *Testes appear firmer, development of a new line of germ cells; grey in color; this stage leads to stage II.* | *SG, PS, SS* |
| *VI. Abnormal* | *a) infection; b) intersex - both female and male tissues can be recognized; c) one lobe degenerated; d) other.* | *e.g. oocytes visible among spermatogenic tissues* |

## 2.7. Batch fecundity

All fish were measured to the nearest 1 mm in the Total Length (TL) and weighted to the nearest 1 g. Gonads of the fish were examined under a dissecting microscope for its external features such as turbidity and color to determine a maturity stage. The sex ratio was also calculated in this study (i.e., No. of males/No. of females (Simon et al., 2012). The female was determined by the macroscopic observation of a mature ovary (Laevastu, 1965). Batch fecundity can vary considerably during the short spawning season, low at the beginning, peaking during high spawning season and declining again towards the end. Annual egg production is the product of the number of batches spawned per year and the average number of eggs spawned per batch. Batch fecundity of sprat was determined using the 'Hydrated Oocyte Method' (Hunter et al., 1985). Oily hydrated females were used. After sampling their body cavity was opened and they were preserved in a buffered formalin solution (Hunter et al., 1985). The ovary-free female weight and the ovary weight were determined. Three tissue samples of ca. 50 mg were removed from different parts of the ovary and their exact weight determined. Under a binocular, the number of hydrated oocytes in each of the three subsamples was determined. Hydrated oocytes can easily be separated from all other types of oocytes because of their large size, their translucent appearance and their wrinkled surface which is due to formalin preservation. Batch fecundity

was estimated based on the average number of hydrated oocytes per unit weight of the three subsamples.
The Gonadosomatic Index (GSI) was determined monthly. GSI was calculated as:

$$GSI = \frac{GW}{SW} X\ 100$$

where GW is gonads weight and SW is the somatic weight (represents the BW without GW)
For the estimation of sprat growth rate, the von Bertalanffy growth function (1938) is used, (according to Sparre, Venema, 1998):

(11) $$L_t = L_\infty \left\{1 - \exp\left[-k\left(t - t_0\right)\right]\right\}$$

(12) $$W_t = W_\infty \left\{1 - \exp\left[-k\left(t - t_0\right)\right]\right\}^n$$

where

$L_t$, $W_t$ are the length and weight of the fish at age *t* years; $L\infty$, $W\infty$ - asymptotic length and weight, $k$ – curvature parameter, $t_o$ - the initial condition parameter.

The length-weight relationship is obtained by the following equation:

(13) $W_t = qL_t^{\ n}$ where $q$ – condition factor, constant in a length-weight relationship; $n$ – constant in a length-weight relationship.

*Coefficient of natural mortality (M)*

Pauly's empirical formula (1979, 1980) was applied:

(14) $$\log M = -0.0066 - 0.279 * \log L_\infty + 0.6543 * \log k + 0.4634 * \log T^{\circ}C$$

(15) $\log M = -0{\cdot}2107 - 0{\cdot}0824 \log W_\infty + 0{\cdot}6757 \log K + 0{\cdot}4627 \log T°C$

where

L∞, W∞ and κ – parameters in von Bertalanffy growth function, T°C - an average annual temperature of the water, ambient of the investigated species.

## 3. Feeding of sprat (*Sprattus sprattus*, L)

**Material and methodology**

The study on the diet of plankton-eating fish (sprat and horse mackerel) in the western part of the Black Sea was based on the analysis of the stomach contents of 60 specimens collected over 2. XI - 10.XI.2022. Additionally, data on the composition and quantity of mesozooplankton in the marine environment were gathered, as this group of organisms forms the main food base of the studied fish species.

The coordinates of the investigated areas and a description of the collected data are listed in Table 3.1.

**Table 3.1.** The research area (2. XI – 10.XI.2022)

| Date | Trawl № | Coordinates | | Depth (m) | Temperature (°C) |
|---|---|---|---|---|---|
| | | Latitude | Longitude | | |
| 2/11/2022 | T 2 | 42.81 | 28.13 | 51 | |
| 3/11/2022 | T 8 | 43.37 | 28.38 | 16 | |
| 5/11/2022 | T 16 | 42.67 | 27.83 | 24 | 16 |
| 8/11/2022 | T 23 | 42.38 | 27.78 | 42 | |
| 9/11/2022 | T 27 | 42.27 | 28.08 | 62 | 17.2 |
| 10/11/2022 | T 32 | 42.44 | 27.91 | 43 | 17.5 |

From the trawl catch, 10/11 live fish specimens were separated and fixed with 10% formaldehyde solution. Under laboratory conditions, the absolute length (TL, with an accuracy of 0.1 cm) and weight (with an accuracy of 0.01 g) of the collected specimens were measured. The stomachs of the studied organisms were weighed using an analytical balance (accuracy, 0.0001 g). The food mass of each fish specimen was calculated as the difference between the weights of the full and empty stomachs.

To determine the species composition of the food and the number of food objects, the stomach contents were examined under a microscope. Prey biomass in fish stomachs was calculated by multiplying the number of zooplankton organisms by their individual weights.

The following indices were defined.

1. Index of stomach fill (ISF) as a percentage of body mass: (weight of stomach contents/weight of fish body) × 100

2. Index of relative importance (IRI; Pinkas et al., 1971): IRI = (N + M) × FO, where N is the proportion of the taxon (species) of the victim in the food by number, M is the proportion of the taxon (species) of the victim in the food by biomass, and FO is the frequency of occurrence of the taxon (species).

Zooplankton samples were collected from the entire water layer (surface–bottom) with a plankton net with an opening diameter d = 36 cm and gas with an aperture of 150 µm, and fixed on board the vessel with a 4% formalin-seawater solution (Korshenko & Aleksandrov, 2013). The species composition of the zooplankton was determined according to the Manuals for the Black and Azov Seas (Mordukhai-Boltovsky et al., 1968) and the quantity in a Bogorov chamber, according to the methodology of Korshenko and Aleksandrov (2013).

## 4. Species diversity

During the research period, 37 trawls were processed in the Bulgarian region of the Black Sea on board the NIC "HaitHabu". The research was carried out in November 2022 (Fig. 4.1.).

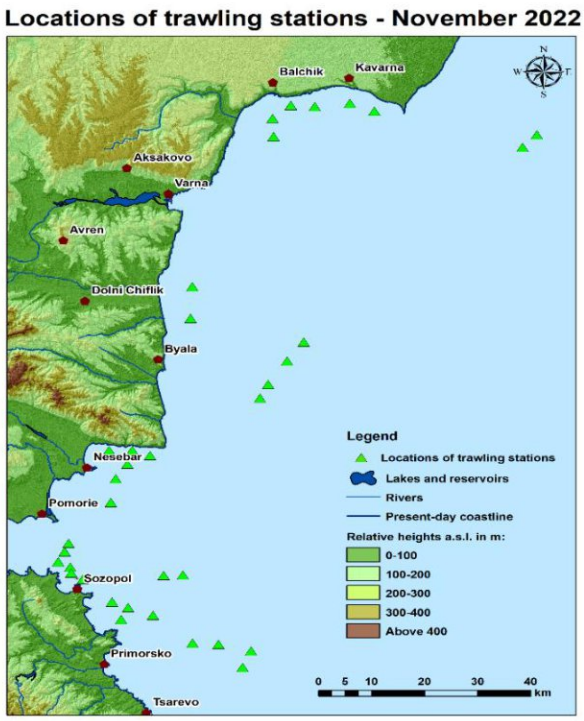

**Figure 4.1.** Sampling stations distribution in November 2022

The trawling operations duration for the study period varied between 30 and 40 minutes at depths between 15 m and 100 m in the area between Ahtopol, Kiten and Durankulak. The presence of sprat in the catch composition has been observed at depths above 18 m.

The total number of species identified during the study was 19, of which 13 fish, 1 crustacean, 2 molluscs and 3 macrozooplankton species. The most frequent species in the trawls (presence/absence) were: *M. merlangius* (26.7%), *M. barbatus* (36.5%) *T. mediterraneus* (16.5%), *S. sprattus* – 59 individuals in 6 trawls, while the other species: *A. immaculata, N. melanostomus, G. niger, M. batrachocephalus, R. clavata, D. pastinaca, P. lascaris, T. draco, S.maximus*, had a negligible presence in the catches.

## 5. Red mullet (*Mullus barbatus* L.)

### 5.1. Distribution

The densest agglomerations of red mullet were registered at depths of 30-50 m with average catch per unit area (CPUA) CPUA = 4432,442 kg.km$^{-2}$ (depth ~30-40 m) in front of Primorsko and Sozopol, Dolni Chiflik and Nessebar, followed by catch per unit area at a depth of 50-100 m (CPUA = 148,335 kg.km$^{-2}$). In the research conducted in November 2022 in the depth layer 15-30 CPUA of red mullet was relatively low - 95 kg.km$^{-2}$.

### 5.2. Red mullet biomass at different depths

In November 2022 the species was caught at 22 of 37 stations. The red mullet biomass in the depth layer 30-50 m was assessed at 8044,085 tonnes, followed by the layer 50-100 m – 408,471 tonnes and 15-30 m – 197,43 tonnes (Fig. 5.2.1.).



*Project № BG14MFOP001-3.003-0004 Collection, management and use of data for the purpose of scientific analysis and implementation of the Common Fisheries Policy for the period 2022, funded by the Maritime and Fisheries Program and co-financed by the European Union through the European Maritime and Fisheries Fund*

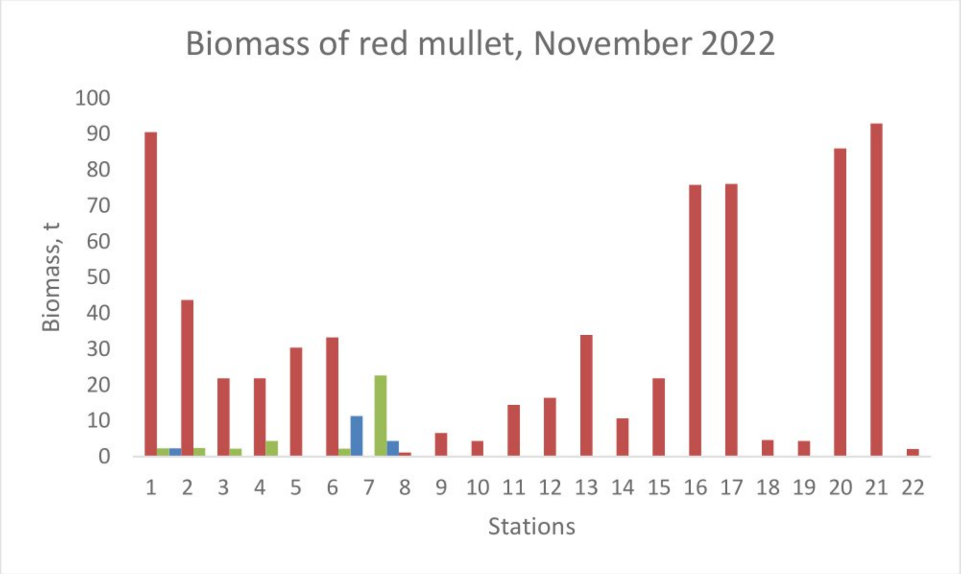


**Figure 5.2.1.** Red mullet biomass at different depth layers Nov. 2022*

*Legend: Green columns: depth stratum 50-75 m Blue columns: depth stratum 15-30 m; Red columns – depth stratum 30-50 m

The biomass at depths of 30-50 m exceeds many times the values in the other depth zones, which indicates optimal conditions for the formation of aggregations precisely at these depths in November 2022 (Table 5.2.1. and 5.2.2.). The studied area is 8010.24 km$^2$ and the total estimated biomass is 8854.217 t.

**Table 5.2.1.** Swept area method implementation in November 2022: mean catch per unit area (CPUA, mean), biomass – in tonnes, Ax-area and number of fields per unit area

| CPUA, mean | Depth | Biomass | Ax area | № of fields |
|---|---|---|---|---|
| | | | | |
| 95,5992 | 15-30 | 197,4257 | 2065,14 | 33 |
| 4432,442 | 30-50 | 8044,085 | 1814,82 | 29 |
| 148,345 | 50-75 | 408,471 | 2753,52 | 66 |
| | | 8854,217 | 8010,24 | 128 |

**Table 5.2.2.** Statistical summary of red mullet biomass indices (t) by depth layers in November 2022

| | 15-30 m | 30-50 m | 50-100 m |
|---|---|---|---|
| **Mean** | 35,849701 | 4230,9 | 127,15288 |
| **Standard error** | 22,596368 | 1235,8 | 64,088212 |
| **Median** | 0 | 445,7 | 36,161438 |
| **Mode** | 0 | 69,8 | #N/A |
| **Standard deviation** | 63,91218 | 5796,7 | 169,56147 |
| **Variance** | 4084,7668 | 33601864 | 28751,092 |
| **Excess** | 4,3698952 | -0,1839349 | -0,8695028 |
| **Asymetry** | 2,0828904 | 1,1563158 | 1,1569139 |
| **Range** | 180,80719 | 17003,357 | 384,05941 |
| **Min** | 0 | 0 | 0 |
| **Max** | 180,80719 | 17003,4 | 384,05941 |
| **Sum** | 286,79761 | 93081,6 | 890,07015 |
| **Count** | 8 | 22 | 7 |
| **Max value (1)** | 180,80719 | 17003,4 | 384,05941 |
| **Min value (1)** | 0 | 0 | 0 |
| **Confidence level (95.0%)** | 53,43192 | 2570,1179 | 156,81821 |

## 5.3. Catch per unit area

The catch per unit area (CPUA $kg.km^{-2}$) was significantly higher in depth layer 30-50 m, where red mulled agglomerations were found. The densest agglomerations were observed in front of (southern) Sozopol and Primorsko; in front of Dolni Chiflik (2 stations) and in the Nessebar Bay (1 station), and in the rest of the investigated areas the species is spatially scattered (Fig. 5.3.1.).

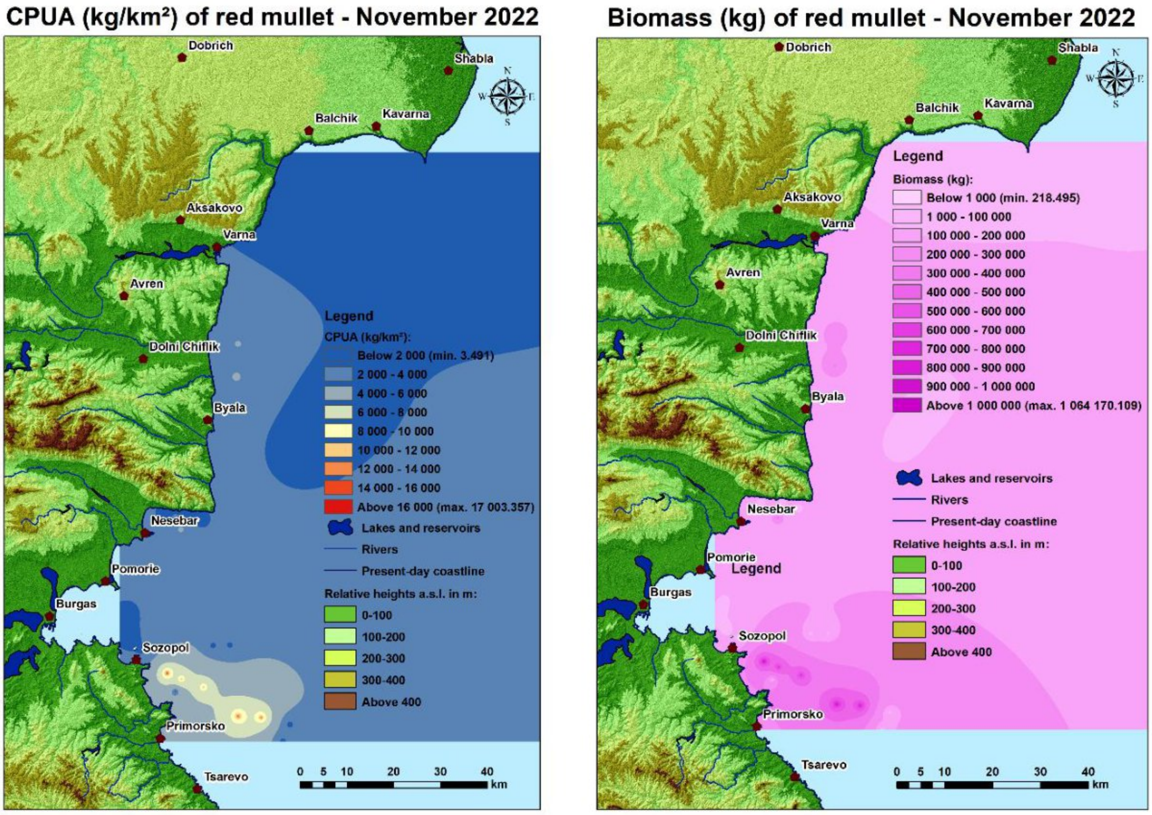


**Figure 5.3.1.** Catch per unit area (CPUA kg.km$^{-2}$ ) and red mullet biomass by depth layers in November 2022

## 5.4. Catch per unit effort

The catch per unit effort (CPUE) for the identified species is graphically represented, spatially identified and analyzed using GIS (Fig. 5.4.1).

The red mullet catch per unit area (CPUE kg.h$^{-1}$) in November 2022 is represented in Fig. 5.4.1.



*Project № BG14MFOP001-3.003-0004 Collection, management and use of data for the purpose of scientific analysis and implementation of the Common Fisheries Policy for the period 2022, funded by the Maritime and Fisheries Program and co-financed by the European Union through the European Maritime and Fisheries Fund*

**CPUE (kg/h) of red mullet - November 2022**

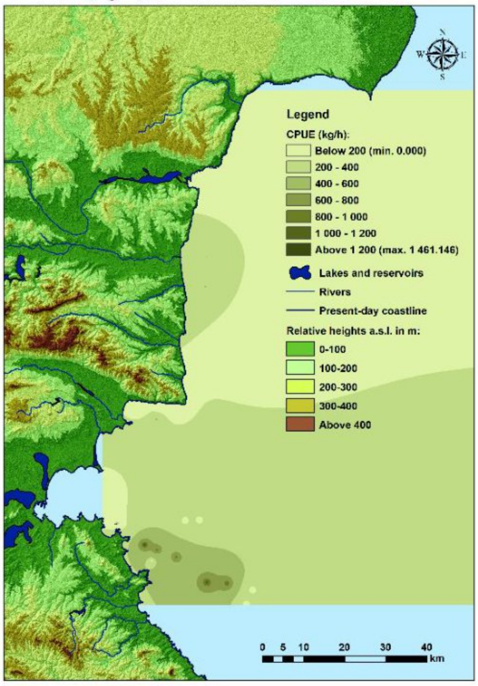


**Figure 5.4.1.** Red mullet catch per unit effort (CPUE), by spatial extent November, 2022

## 5.5. Length-weight relationship (LWR) of red mullet

The LWR in red mullet is best described by the model: $W = 0.00575.L^{3,23}$, showing positive allometric growth ($\geq 3$), the resulting nonlinear model has a high degree of statistical determination (R2 = 0.9973) (Fig. 5.5.1.).

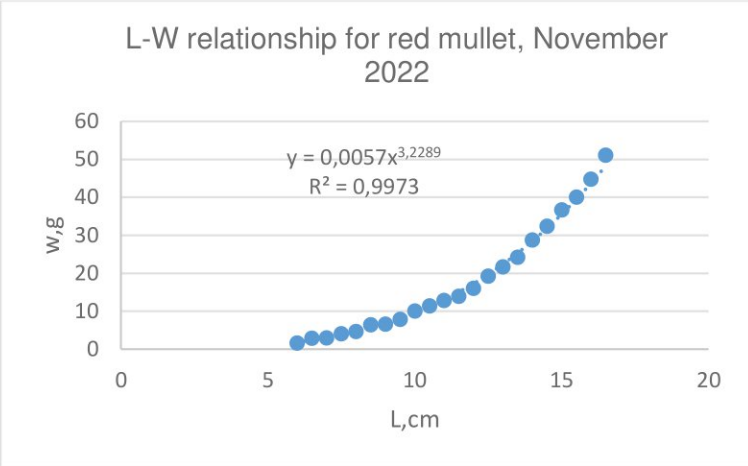


**Figure 5.5.1.** Red mullet LWR model in November 2022

The size structure of the red mullet stock is presented in Figure 5.5.2. During the study, the smallest observed size class was 6 cm and the largest was 16.5 cm, with predominant size classes in the catch composition 11-12 cm. The other size classes were less represented.

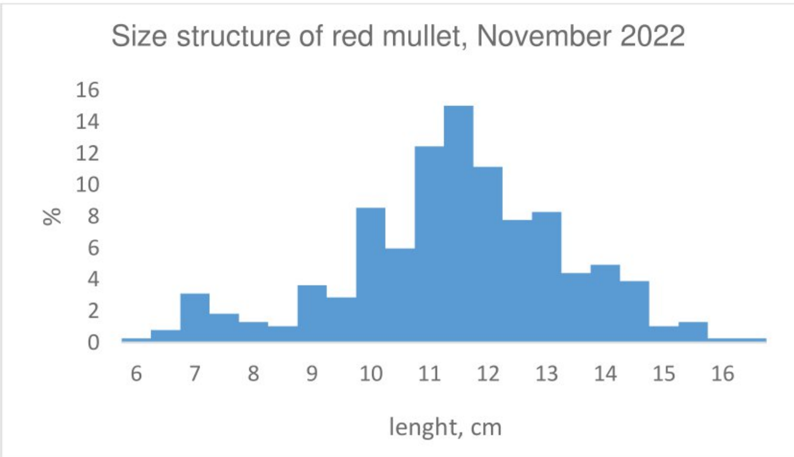


**Figure 5.5.2.** Length composition of red mullet represented in the survey carried out in November 2022

The species was recorded in almost all control trawls in November 2022, indicating the presence of dense aggregations in the studied areas.

## 6. Whiting (*Merlangius merlangus*)

### 6.1. Distribution

The whiting inhabits the bottom deep layers and its main food is sprat. The species is carnivorous and is an important component of the food chain of other larger predators such as turbot and dolphins. The whiting is significantly represented in the catches.

### 6.2. Whiting biomass by stratums

The highest average value of the whiting biomass was observed in the 15-30 m layer: 2935.731 t. In the remaining two depth layers 30-50 m and 50-100 m the biomass values were 1985.366 and 655.4191t. The spatial distribution of the whiting was scattered, with higher abundances found in the 30-50m stratum, opposite Obzor, Banya village, Arkutino/ Primorsko and south of Sozopol (Fig. 6.2.1).

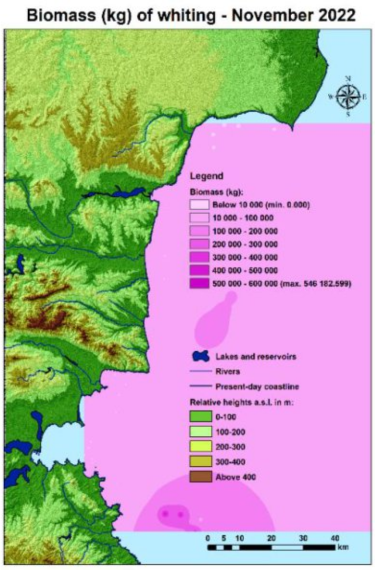


**Figure 6.2.1.** Biomass of whiting in the different depth layers, November 2022



*Project № BG14MFOP001-3.003-0004 Collection, management and use of data for the purpose of scientific analysis and implementation of the Common Fisheries Policy for the period 2022, funded by the Maritime and Fisheries Program and co-financed by the European Union through the European Maritime and Fisheries Fund*

The total studied area was 8010.24 km$^2$, and the total biomass of the whiting was assessed up to 5576,516 tons (Table 6.2.1, Table 6.2.2 and Fig. 6.2.2).

**Table 6.2.1.** Swept Area method for stock assessment survey in November 2022 - average values of catch per unit area (CPUA), biomass (kg), Ax - area and number of fields

| CPUA, mean | Depth | Biomassa | Ax area | № of fields |
|---|---|---|---|---|
| 1421,565 | 15-30м | 2935,731 | 2065,14 | 33 |
| 1093,974 | 30-50м | 1985,366 | 1814,82 | 29 |
| 158,6864 | 50-100м | 655,4191 | 4130,28 | 66 |
| | | | 8010,24 | 128 |

The species was observed at 22 of 37 total examined in the research.

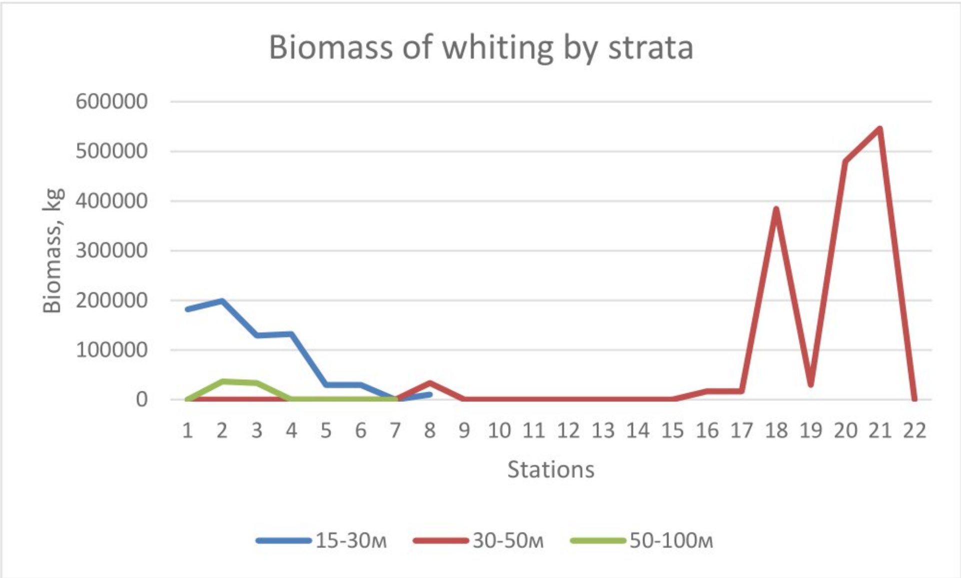


**Figure 6.2.2.** Biomass (kg) of whiting by strata in November 2022

**Table 6.2.2. Descriptive statistics of the CPUA indices (t) of whiting in November 2022**

| | 15-30 m | 30-50 m | 50-100 m |
|---|---|---|---|
| **Mean** | 1421,565 | 1093,974 | 158,6864 |
| **Standard Error** | 454,7425 | 564,0112 | 102,5941 |
| **Median** | 1269,491 | 0 | 0 |
| **Mode** | 476,0591 | 0 | 0 |
| **Standard Deviation** | 1286,206 | 2645,447 | 271,4384 |
| **Sample Variance** | 1654326 | 6998390 | 73678,8 |
| **Kurtosis** | -2,02477 | 4,201745 | -0,75517 |
| **Skewness** | 0,241056 | 2,365791 | 1,243227 |
| **Range** | 3173,727 | 8727,75 | 581,85 |
| **Minimum** | 0 | 0 | 0 |
| **Maximum** | 3173,727 | 8727,75 | 581,85 |
| **Sum** | 11372,52 | 24067,43 | 1110,805 |
| **Count** | 8 | 22 | 7 |
| **Largest(1)** | 3173,727 | 8727,75 | 581,85 |
| **Smallest(1)** | 0 | 0 | 0 |
| **Confidence Level (95,0%)** | 1075,295 | 1172,925 | 251,0386 |

## 6.3. Catch per unit area

The whiting was presented in the composition of the catches during the first part part of the expedition, conducted in November 2022 with the highest distribution density of the species, registered in the region of Arkutino (Fig. 6.3.1.). The species was detected at 22 stations from 37 in total.



*Project № BG14MFOP001-3.003-0004 Collection, management and use of data for the purpose of scientific analysis and implementation of the Common Fisheries Policy for the period 2022, funded by the Maritime and Fisheries Program and co-financed by the European Union through the European Maritime and Fisheries Fund*

In the depth layer 30-50 m, the highest recorded value for CPUA was 8727,75 kg.km$^{-2}$, with an average CPUA value - 1093,974 kg.km$^{-2}$. In the depth layer 15-30 m, 3173,727 kg.km$^{-2}$ and average CPUA value 1421,565 kg.km$^{-2}$, the species was registered during all experimental trawls (Fig. 6.3.1.). 1421; 50-100 m – 581,85 kg.km$^{-2}$ and average CPUA value: 158,6864 kg.km$^{-2}$, the species was registered during all experimental trawls (Fig. 6.3.1.).

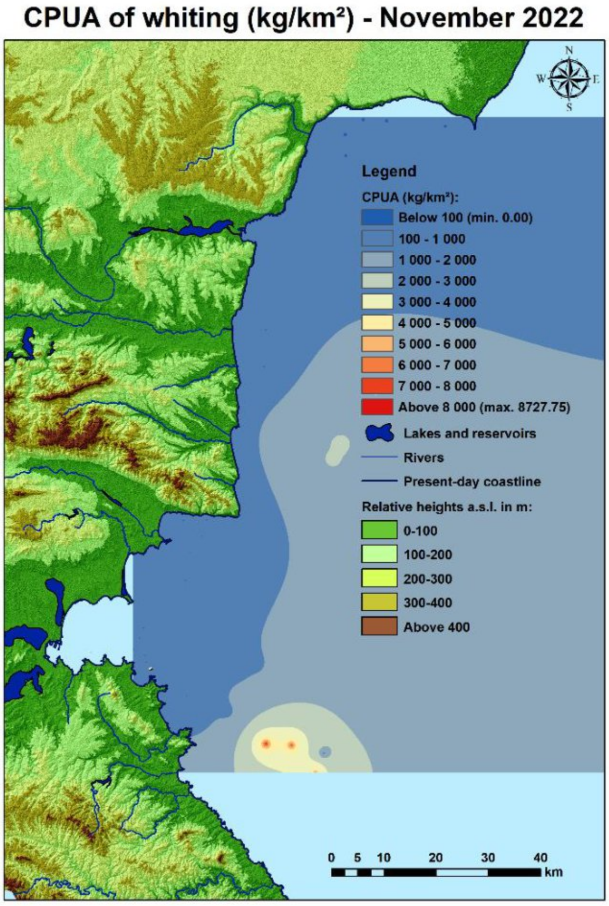


**Figure 6.3.1.** Catch per unit area (CPUA kg.km$^{-2}$ ), November 2022

## 6.4. Catch per unit effort

The catch per unit effort (CPUE) for the species is presented graphically on Fig. 6.4.1.The highest CPUE (kg.h$^{-1}$) were observed in front of Arkutino.



*Project № BG14MFOP001-3.003-0004 Collection, management and use of data for the purpose of scientific analysis and implementation of the Common Fisheries Policy for the period 2022, funded by the Maritime and Fisheries Program and co-financed by the European Union through the European Maritime and Fisheries Fund*

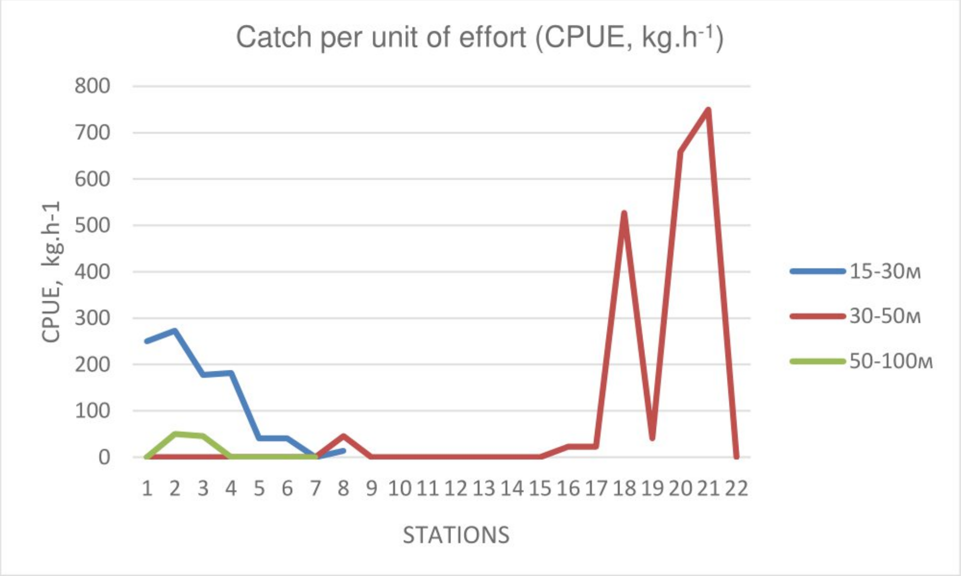


**Figure 6.4.1.** Catch per unit effort (CPUE kg.$h^{-1}$ ) of whiting in November, 2022

## 6.5. Length - weight relationship

The length-weight relationship of the whiting is described by the model W = $0.0711.L^{2.19}$, the coefficient of allometric growth ≤ to 3, the obtained nonlinear model of the length-weight relationship is a high degree of determinism (R2 = 0.943) (Fig. 6.5.1).

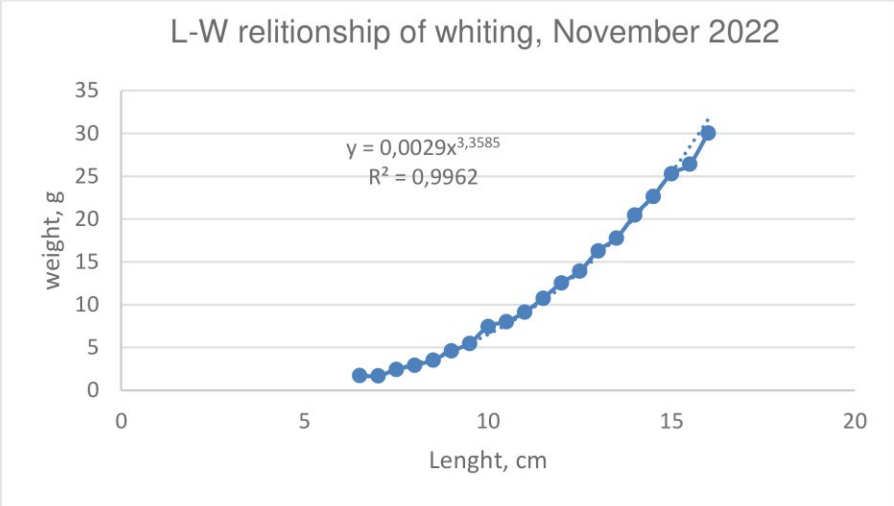


**Figure 6.5.1.** Length-weight relationships of whiting in November 2022

The size structure of the whiting stock is presented in Fig.6.5.2. The length distribution in the whiting samples was bimodal, with peaks at 11.5-12.5 and 14-14.5 cm. A peak was observed in the 14 cm size group.

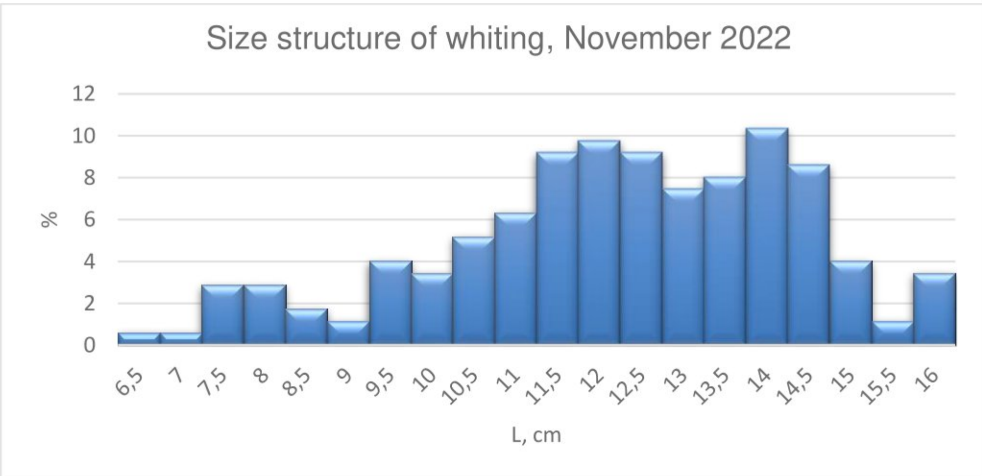


**Figure 6.5.2.** Size structure of whiting November, 2022

# 7. Horse mackerel

## 7.1. Distribution

The horse mackerel is a migratory species in front of the Bulgarian coast. In November 2022, the species formed dense aggregations in the deep layers.

## 7.2. Biomass of horse mackerel by strata

The highest average biomass values were recorded in the 30-50m layer (1059,066 tons, east of Primorsko), followed by 1006,503 tons in the 50-100m layer. At depths of 15-30m, we observed the smallest accumulations of horse mackerel - 138.09 tons. The total biomass established in November 2022 was 2203.66 tons (Table 7.2.1., Table 7.2.2., Fig. 7.2.1 and Fig. 7.2.2).

**Table 7.2.1.** Area method for investigation of stocks in November 2022, average catch per unit area (CPUA), Biomass (kg), Ax-area and number of fields per area

| av.CPUA | depths | Biomassa | Ax Surface | No. stations |
|---|---|---|---|---|
| 66,86749 | 15-30м | 138,0907 | 2065,14 | 33 |
| 583,5653 | 30-50м | 1059,066 | 1814,82 | 29 |
| 243,6889 | 50-100м | 1006,503 | 4130,28 | 66 |
| | | 2203,66 | 8010,24 | 128 |

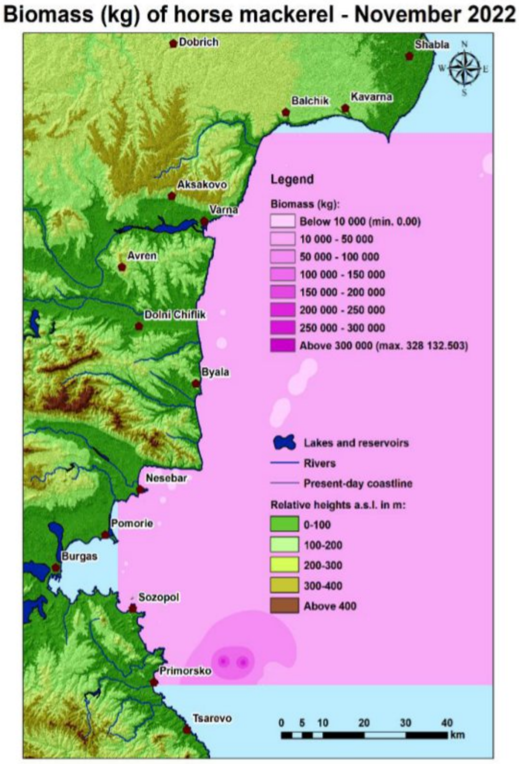


**Figure 7.2.1.** Horse mackerel biomass from the deep layers of the study areas in November, 2022

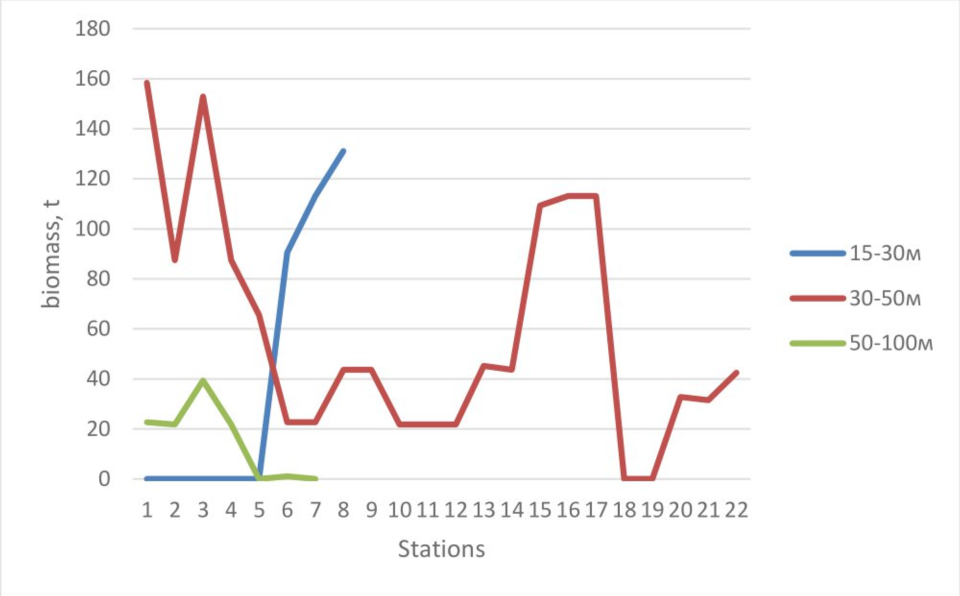


**Figure 7.2.2.** Biomass (kg) of horse mackerel by strata in November 2022

**Table 7.2.2.** Descriptive statistics of the CPUA indices (t) of horse mackerel in November 2022

| | **15-30 m** | **30-50 m** | **50-100 m** |
|---|---|---|---|
| **Mean** | 66,86749 | 583,5653 | 15,25005 |
| **Standard Error** | 33,20078 | 316,0746 | 5,746492 |
| **Median** | 0 | 88,53318 | 21,84949 |
| **Mode** | 0 | 69,82898 | 21,84949 |
| **Standard Deviation** | 93,90598 | 1482,521 | 15,20379 |
| **Sample Variance** | 8818,333 | 2197869 | 231,1552 |
| **Kurtosis** | -1,7307 | 7,898536 | -1,10934 |
| **Skewness** | 0,771876 | 3,0117 | 0,332418 |
| **Range** | 209,487 | 5243,408 | 39,32908 |
| **Minimum** | 0 | 0 | 0 |

| | | | |
|---|---|---|---|
| **Maximum** | 209,487 | 5243,408 | 39,32908 |
| **Sum** | 534,9399 | 12838,44 | 106,7504 |
| **Count** | 8 | 22 | 7 |
| **Largest(1)** | 209,487 | 5243,408 | 39,32908 |
| **Smallest(1)** | 0 | 0 | 0 |
| **Confidence Level (95,0%)** | 78,50736 | 657,3131 | 14,06116 |

## 7.3. Catch per unit area

At depths of 30-50m, in two of the studied stations, peaks in the catch per unit area of 5243.408 and 5039.589 kg.km$^{-2}$ in front of Primorsko were established (Fig. 7.3.1). In other stations, the variation of the catch per unit area was in a wide range from 17 to 628 kg.km$^{-2}$. Average values by stratum were as follows: 15-30m: 66.87 kg.km$^{-2}$; 30-50m: 584 kg.km$^{-2}$; 50-100m: 244 kg.km$^{-2}$.

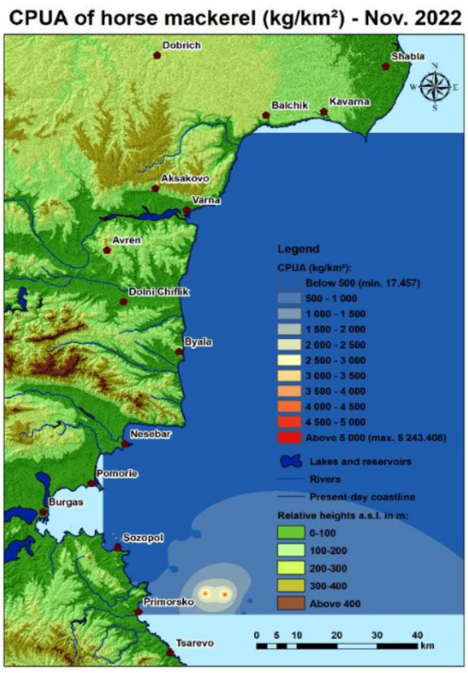


**Figure 7.3.1.** Catch per unit area (CPUA kg.km$^{-2}$ ) of horse mackerel from the different deep layers in November, 2022

### 7.4. Catch per unit effort

At depths of 30-50m, in two of the studied stations, peaks were established (in front of Primorsko) in the catch per unit of effort (CPUE = 438 and 435 kg.h$^{-1}$). In the other stations, the parameter was significantly lower.

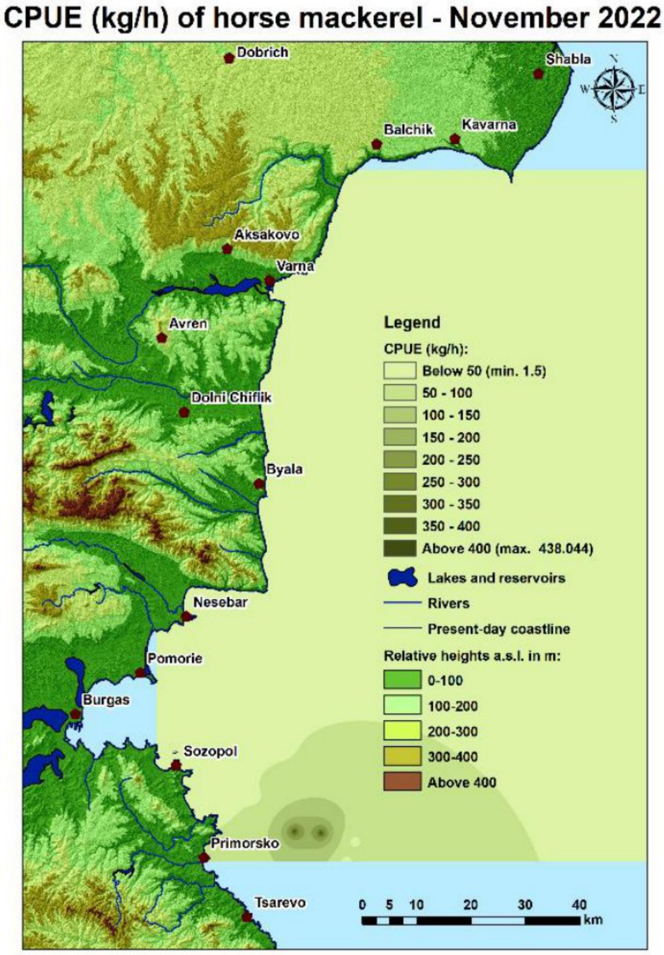


**Figure 7.4.1.** Catch per unit effort (CPUE kg.h$^{-1}$) of sprat from the different deep layers in November, 2022

### 7.5. Length – weight relationship

The length-weight relationship of the horse mackerel is described by the model $W= 0.0029.L^{3,35}$, the coefficient of allometric growth ≥ to 3, the obtained nonlinear model of the length-weight relationship is a high degree of determinism (R2 = 0.99) (Fig. 7.5.1.).

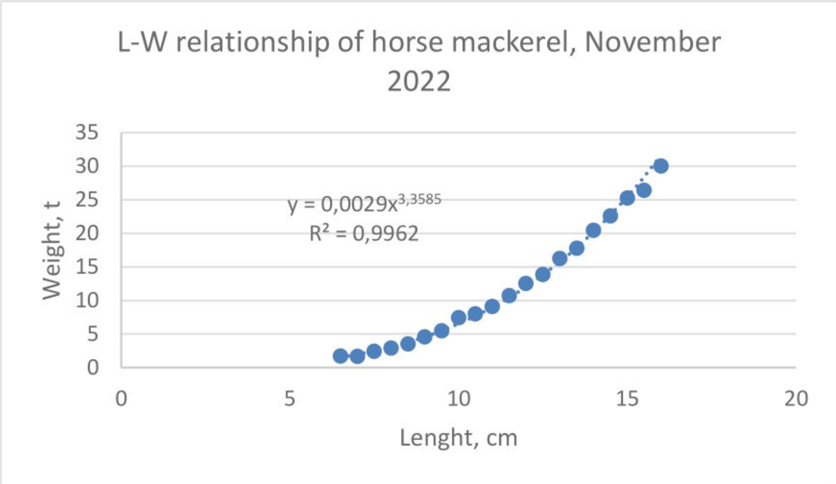


**Figure 7.5.1.** Length-weight relationships of horse mackerel in November, 2022

The size structure of the horse mackerel stock is shown in Figure 7.5.2. The length distribution in the horse mackerel samples was bimodal, with peaks at 12.5 and 14 cm (Fig. 7.5.2.).

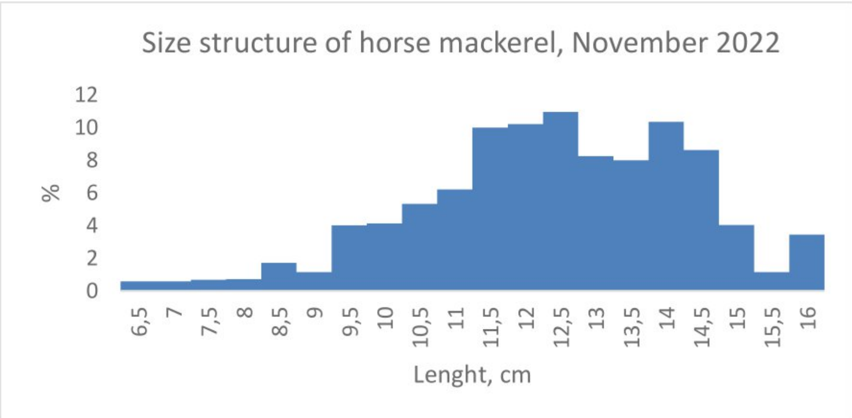


**Figure 7.5.2.** Size structure of horse mackerel, November 2022



*Project № BG14MFOP001-3.003-0004 Collection, management and use of data for the purpose of scientific analysis and implementation of the Common Fisheries Policy for the period 2022, funded by the Maritime and Fisheries Program and co-financed by the European Union through the European Maritime and Fisheries Fund*

## 8. Species poorly represented in catches

Anchovy (*E. encrasicolus* L.) - although the species among the most widespread pelagic species in the Black Sea, during the study period it was represented with zero catches. The species did not form dense aggregations that prevent its capture with active trawl devices; The combination of the presence of predatory fish species and dolphins further disperses the anchovy flocks and makes it difficult to get into the trawling gears as well.

Gobies - three species were observed in the catches. The quantitative assessment was not possible due to the small number of different species in the separate hauls.

Single specimens of *A. immaculata* were also identified during the trawls.

## 9. Age structure

The predominant age group of sprat (n = 59) during the he study period was 1-1+ (46.6%), followed by 2-2+ (33%). The recruitment was presented with 2.55%. The age structure of the whiting varied from 0 to 5 + years with the highest representation of the age group 4+. The distribution of the age groups of the red mullet was similar, and as of the whiting the recruitment was presented with a smaller share (~%). Red mullet age structure was represented by 5 age groups, as the prevailing age class was 2-2+ $y^{-1}$ (Fig. 9.1). Horse mackerel prevailing age class was 2-2+$y^{-1}$. The percentage of the 1-1+ and 3-3+ was as two fold less than 2 years olds.



*Project № BG14MFOP001-3.003-0004 Collection, management and use of data for the purpose of scientific analysis and implementation of the Common Fisheries Policy for the period 2022, funded by the Maritime and Fisheries Program and co-financed by the European Union through the European Maritime and Fisheries Fund*

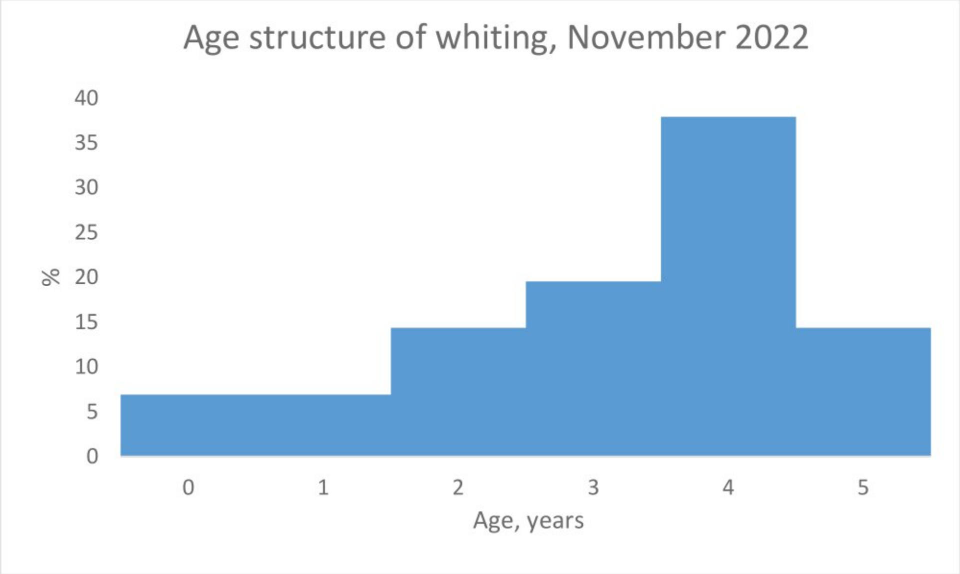
Age structure of whiting, November 2022
%
0
5
10
15
20
25
30
35
40
0
1
2
3
4
5
Age, years

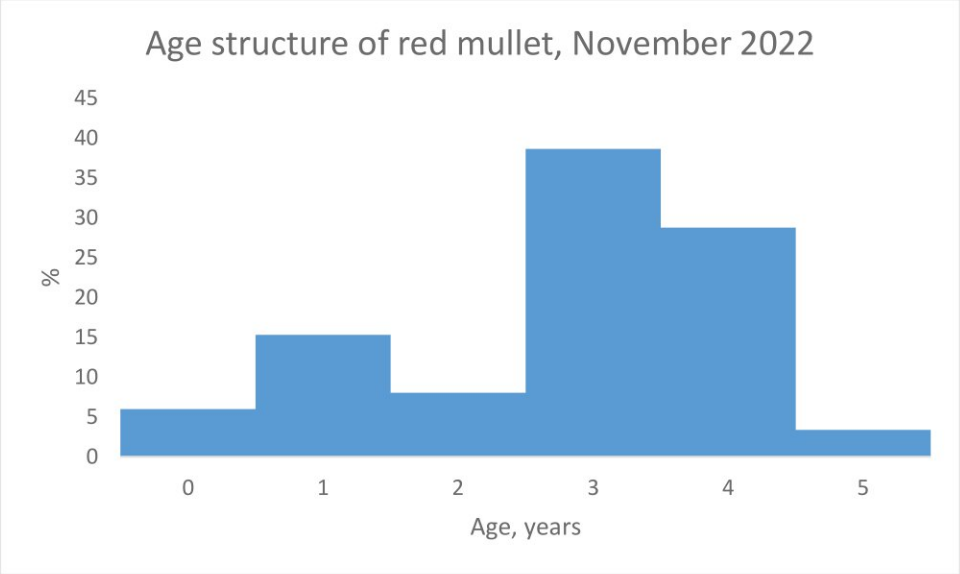
Age structure of red mullet, November 2022
%
0
5
10
15
20
25
30
35
40
45
0
1
2
3
4
5
Age, years

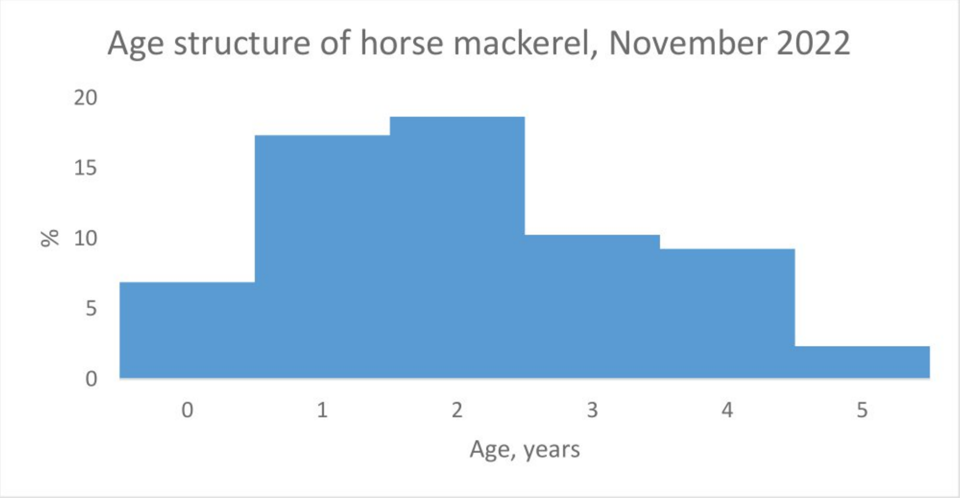


**Figure 9.1.** Age structure of the studied species in November 2022

## 10. Individual growth

The low number of sprat individuals caught in November 2022 (n=59) did not allow calculation of asymptotic length and growth parameters. Whiting and horse mackerel are characterized by lower growth rates, but a relatively high value of asymptotic length, similar to the red mullet, with the exception of horse mackerel, due to the low number of examined and caught individuals (Table 10.1.).

**Table 10.1.** Von Bertalanffy growth model (VBGF) for sprat, whiting, red mullet and horse mackerel

| Species | Asyptotic lenght | Growth rate | Growth parameter | Growth coefficient | Allometric coefficient |
|---|---|---|---|---|---|
| *S. sprattus* | L∞ = 12.44* | k=0.4* | t0 = -1.012* | q = 0.008* | n = 2.33* |
| *M. merlangus* | L∞ = 28.1 | к=0.25 | t0 = -2.0125 | q = 0.009 | n = 2.20 |
| *M. barbatus* | L∞ = 18.81 | к=0.25 | t0 = -1.333 | q = 0.009 | n = 3.22 |
| *Tr. mediterraneus* | L∞ = 18.3 | к=0.33 | t0 = -1.11 | q = 0.008 | n = 1.024 |

*Growth parameters from the autumn-winter study, 2022

### 10.1. Somatic growth

The average weights of the whiting, red mullet and horse mackerel by age groups are presented in Figure. 10.1.1. No somatic growth calculations were possible for the sprat due to the low number of specimens caught in November 2022.

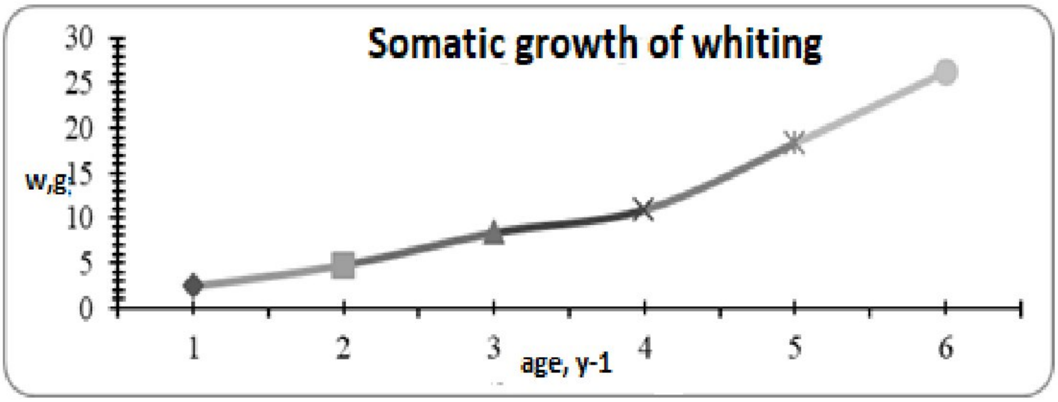


a

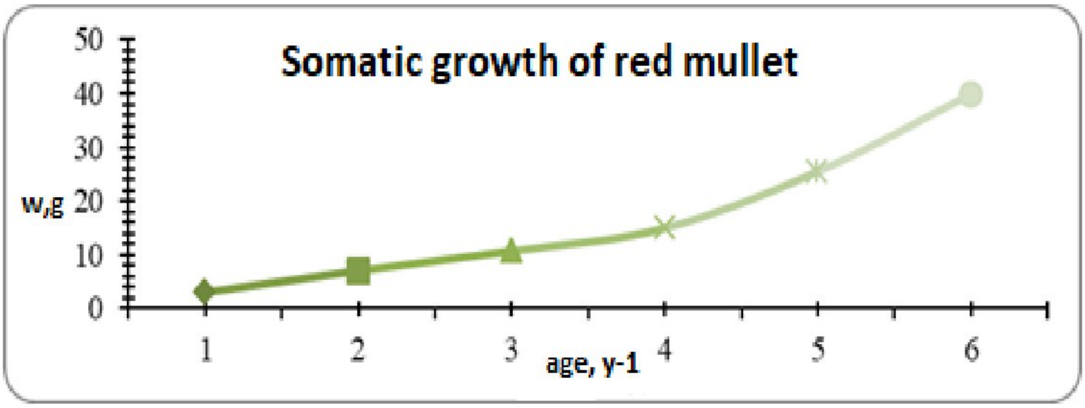


b

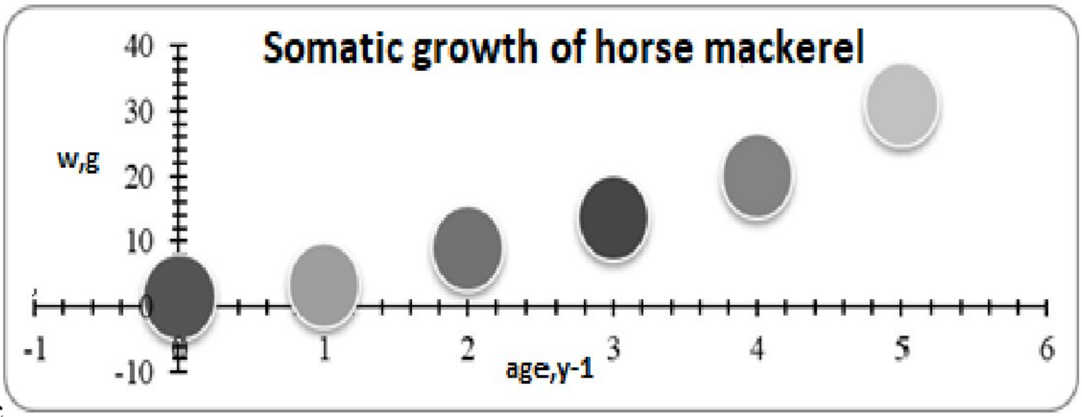


c

**Figure 10.1.1.** Somatic growth of November 2022: a) whiting, b) red mullet, c) horse mackerel

## 11. Catch numbers

Abundance and biomass (by size and age) of sprat in the catches could not be calculated due to the low number of specimens from 4 trawl stations in November 2022.

In terms of abundance of red mullet, the predominant size classes present in the catches were 7, 10, 11 and 11.5 cm (Fig. 11.1.). The peak of red mullet biomass was observed in size classes 7, 10, 11.5 - 12 cm (Fig. 11.2.).

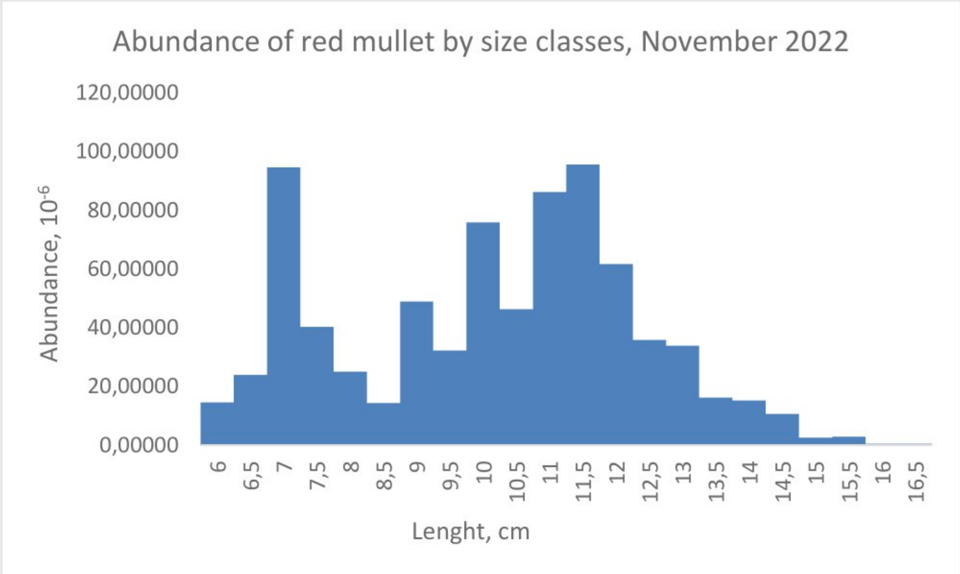


**Figure 11.1.** Abundance of red mullet by size classes in November 2022

The analysis of biomass distribution by age groups showed the highest values for age group 3+ and 4+ year specimens (Fig. 11.2.).

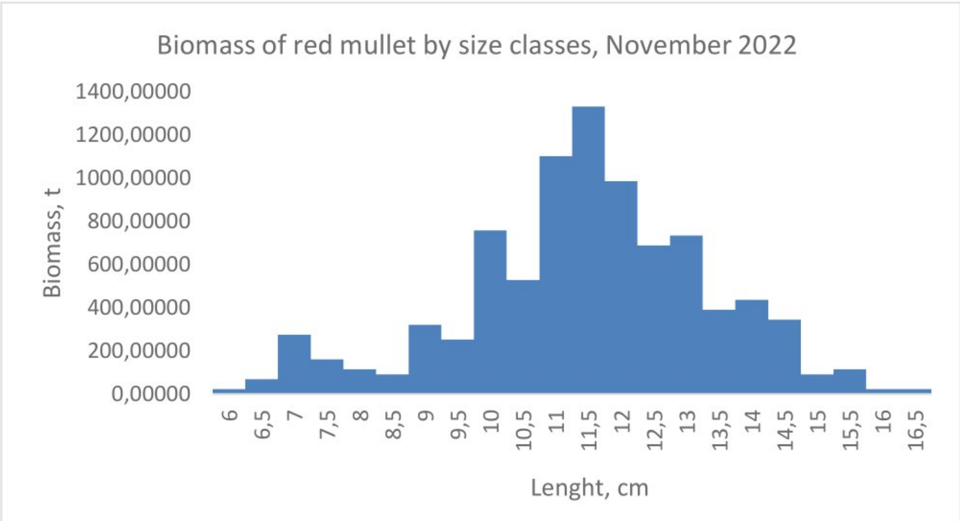


**Figure 11.2.** Biomass of red mullet by size classes in November 2022

The abundance of red mullet by age in November 2022 showed peaks of 1-1+ and 3-3+ years (Fig. 11.3).

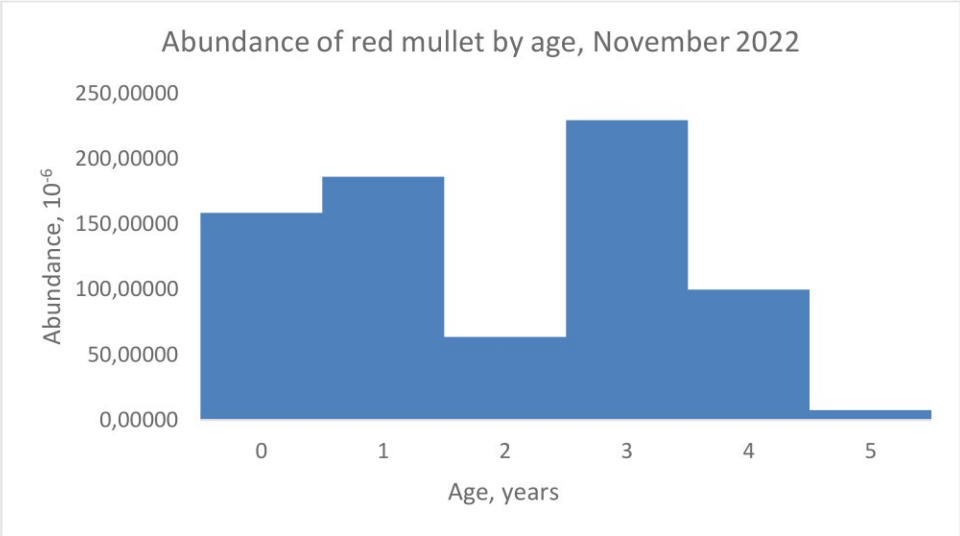


**Figure 11.3.** Abundance of red mullet by age in November 2022

Red mullet biomass by age in November 2022 showed a peak at 3-3+ year old, followed by 4-4+ year old (Fig. 11.4).

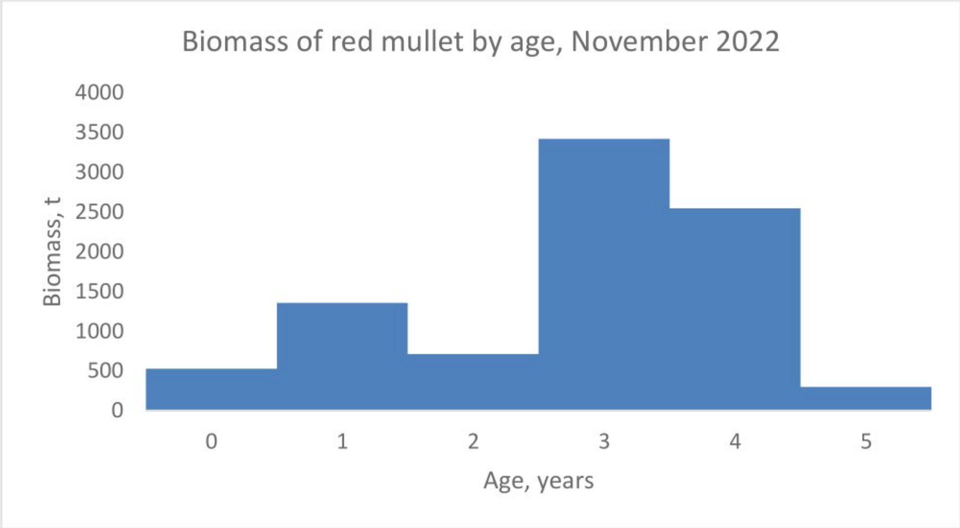


**Figure 11.4.** Biomass of red mullet by age classes in November 2022

The highest numbers of representation in the catches were for size classes 11.5 – 12.5 cm with maximum for 14 cm (Fig. 11.5).

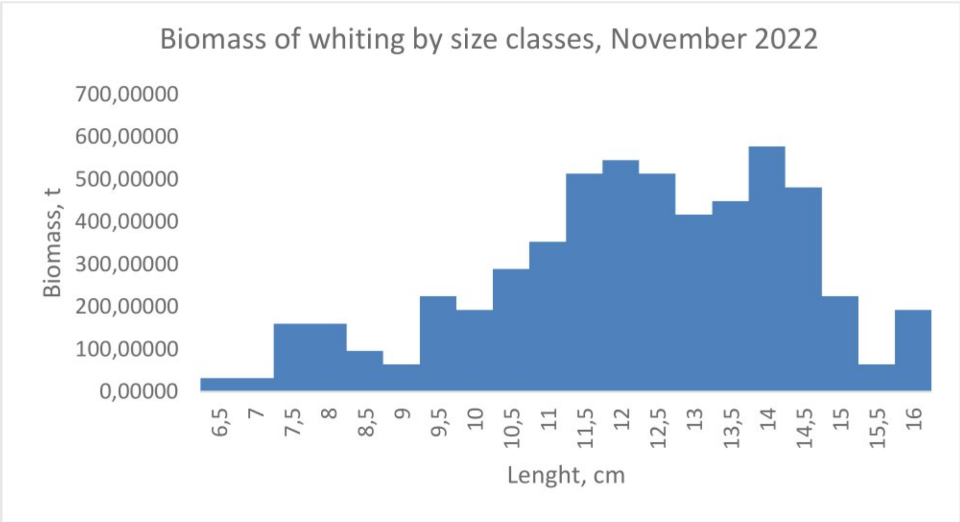


**Figure 11.5.** Biomass of whiting by size classes in November 2022



*Project № BG14MFOP001-3.003-0004 Collection, management and use of data for the purpose of scientific analysis and implementation of the Common Fisheries Policy for the period 2022, funded by the Maritime and Fisheries Program and co-financed by the European Union through the European Maritime and Fisheries Fund*

The most abundant age classes of whiting were 1 and 4 years, with age classes 0+ и 5 characterized by low abundance indices in November 2022 (Fig. 11.6.).

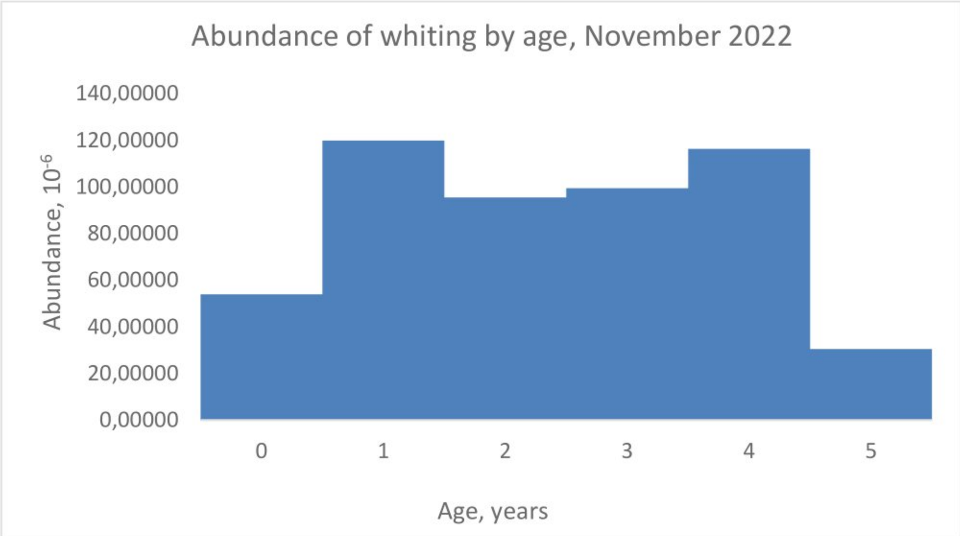


**Figure 11.6.** Abundance of whiting by age classes in November 2022

In November 2022 the highest share of the horse mackerel was for size classes 8,5, 9.5 и 12 - 12.5 cm (Fig. 11.7). The largest number is in the age group 1+ years and 0+ years (Fig. 11.8.).

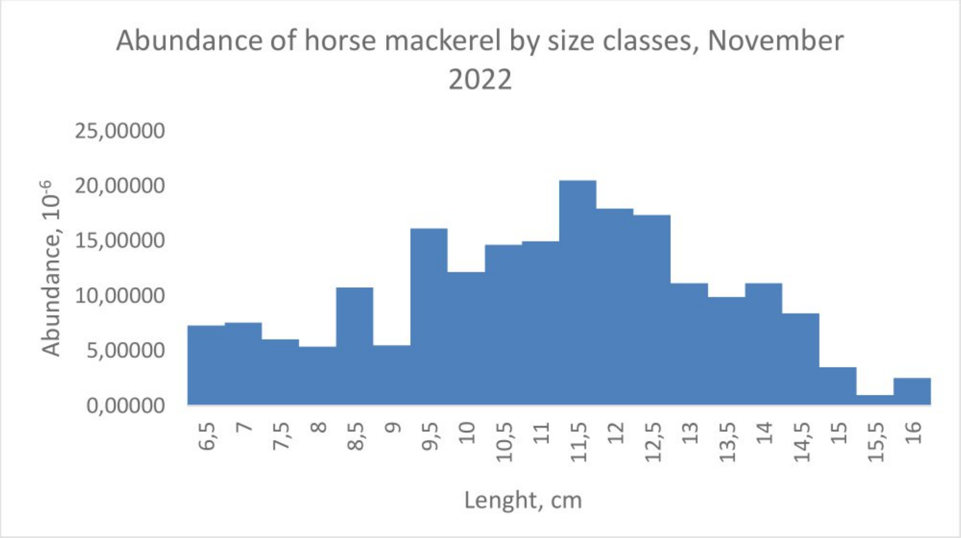


**Figure 11.7.** Abundance of horse mackerel by size classes in November 2022

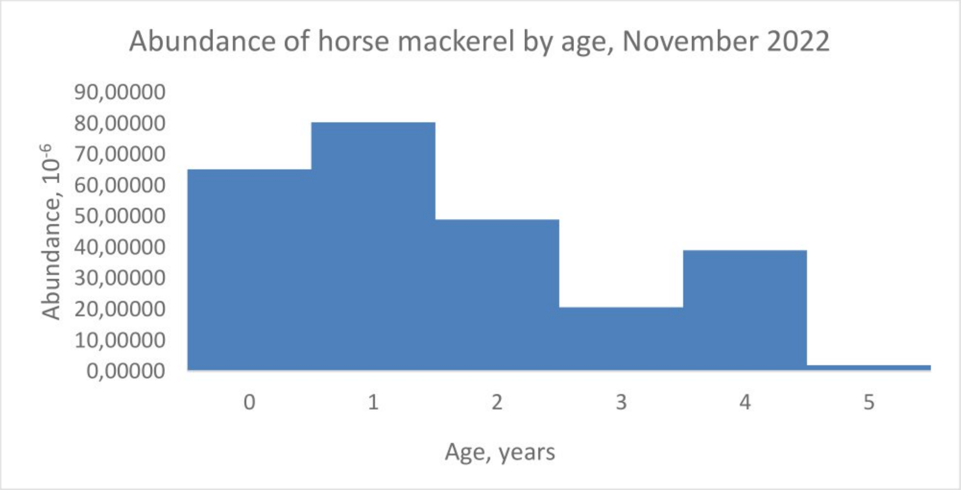


**Figure 11.8.** Abundance of horse mackerel by age classes in November 2022

Biomass of horse mackerel was relatively low for size classes 6.5 to 9 cm and for 15.5 cm, with the highest values for 1.5-12.5, 14 and 14.5 cm (Fig. 11.9.) and age classes 1-1+ and 4+ years (Fig. 11.10.).

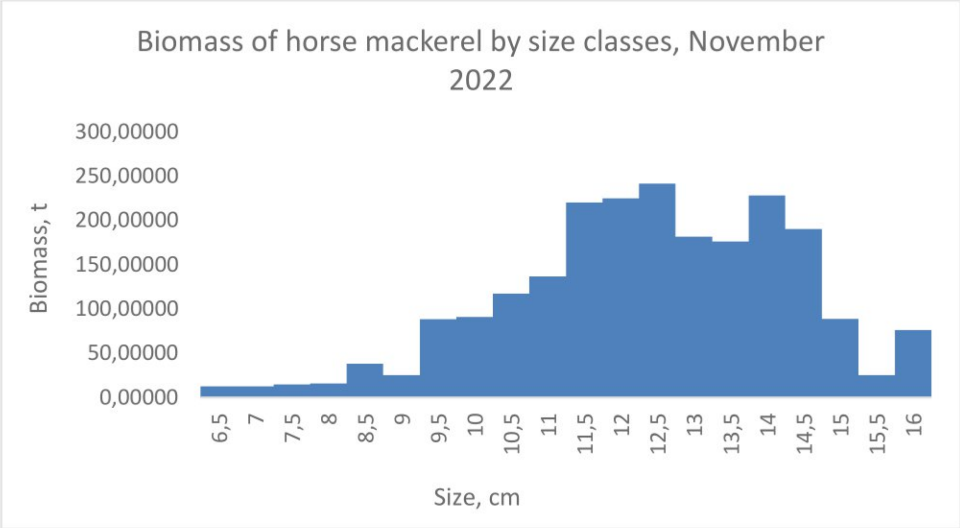


**Figure 11.9.** Biomass of horse mackerel by size classes in November 2022

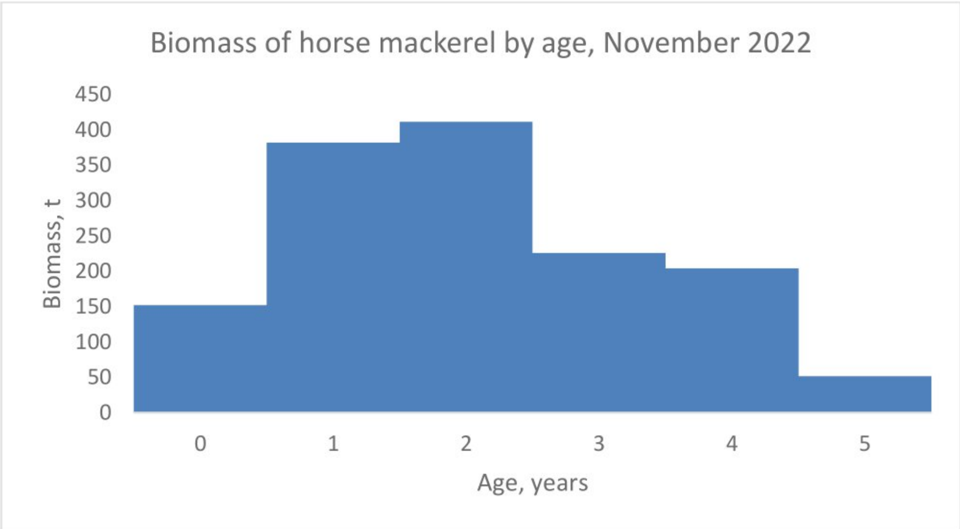


**Figure 11.10** Biomass of horse mackerel by age classes in November 2022

## 12. Sex ratio and maturity

Females and males of the sprat, whiting, horse mackerel and red mullet were represented with a percentage of 49:48%; 49:49%; 50:49%; 48:51%. The juveniles were represented by a very small percentage (1-3%) (Fig. 12.1).

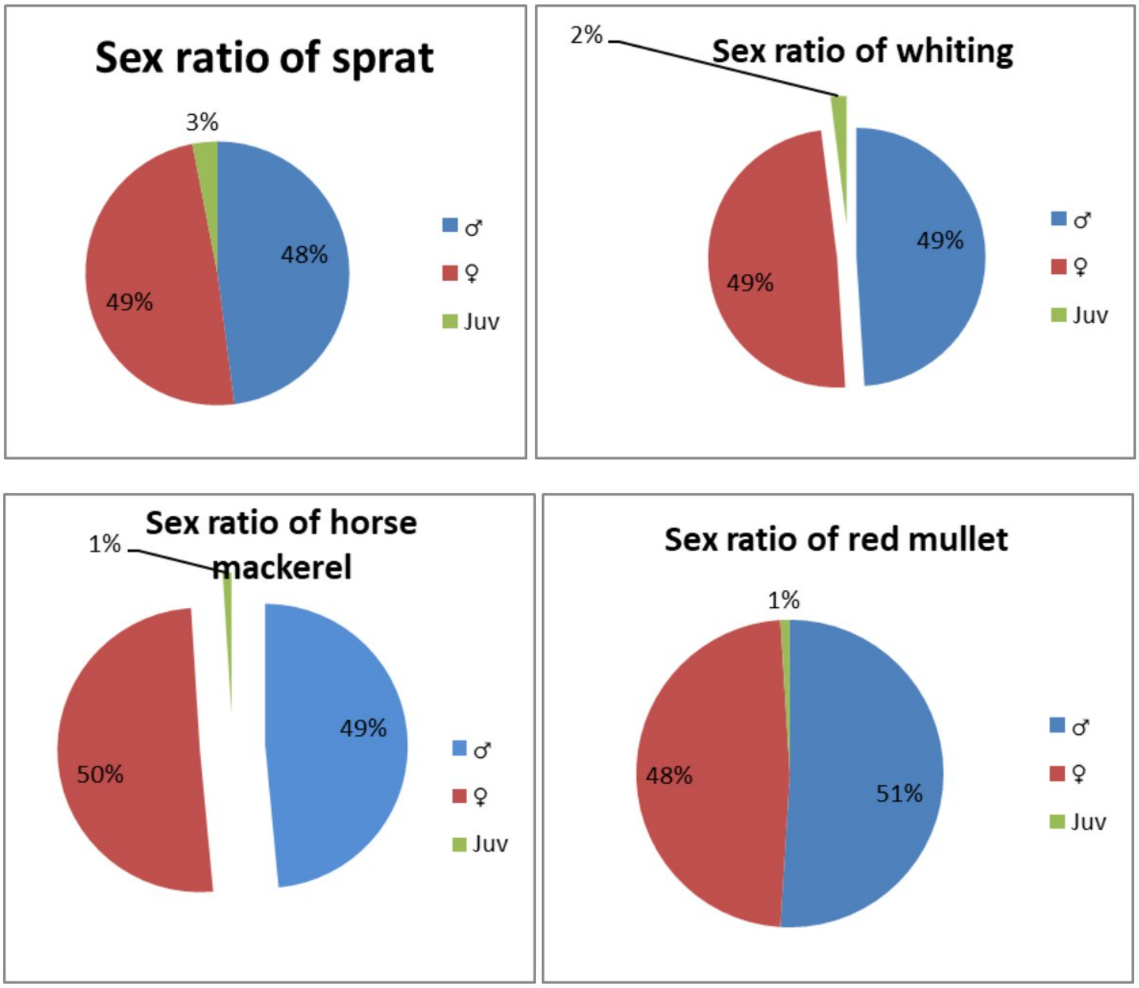


**Figure 12.1.** Sex ratio (females - ♀, males - ♂ and juveniles - Juv) of the studied species



*Project № BG14MFOP001-3.003-0004 Collection, management and use of data for the purpose of scientific analysis and implementation of the Common Fisheries Policy for the period 2022, funded by the Maritime and Fisheries Program and co-financed by the European Union through the European Maritime and Fisheries Fund*

The sexual maturity of the analyzed species by size classes is presented in Fig.12.2., and according to the age groups in Fig.12.3.

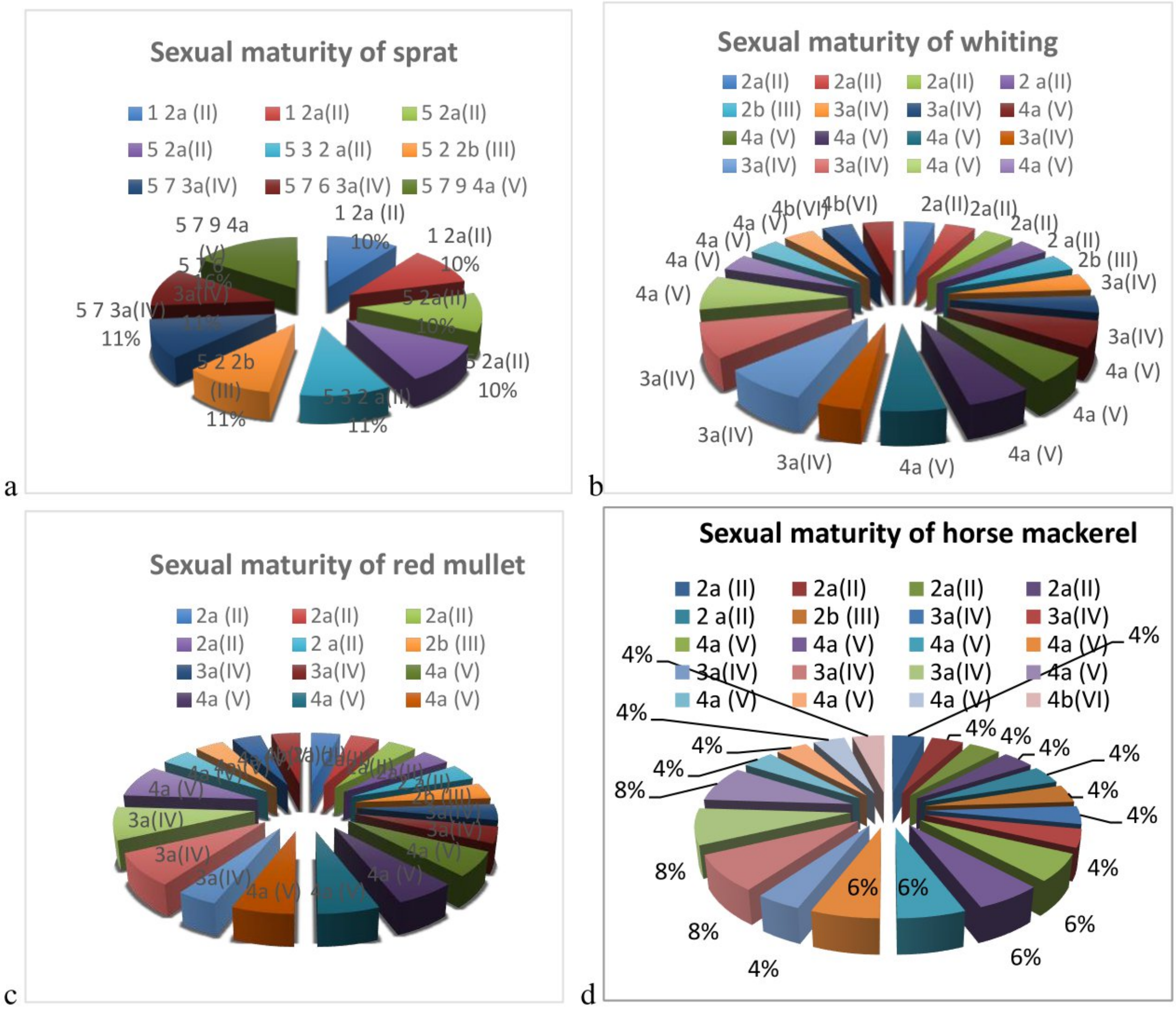


**Figure 12.2.** Sexual maturity of the studied species analysed by size classes a) sprat b) whiting c) red mullet d) horse mackerel

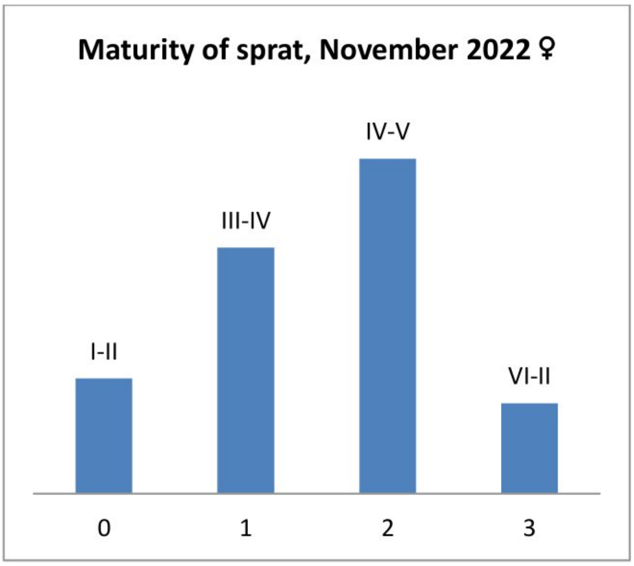
Maturity of sprat, November 2022 ♀
I-II
III-IV
IV-V
VI-II
0
1
2
3

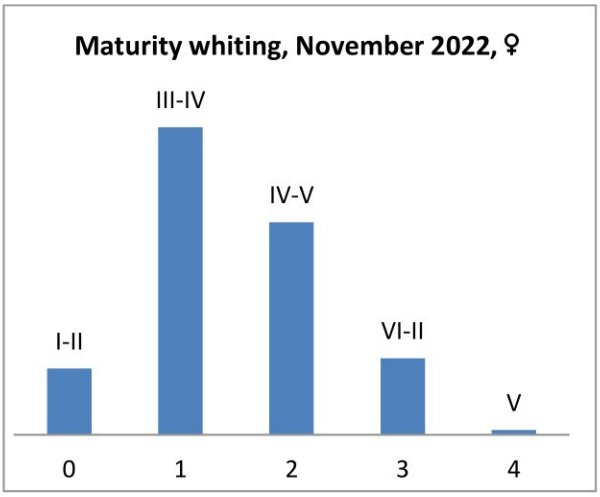
Maturity whiting, November 2022, ♀
I-II
III-IV
IV-V
VI-II
V
0
1
2
3
4

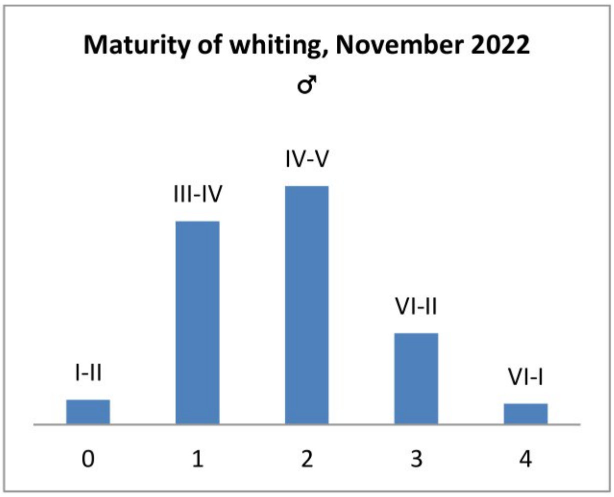
Maturity of whiting, November 2022 ♂
I-II
III-IV
IV-V
VI-II
VI-I
0
1
2
3
4

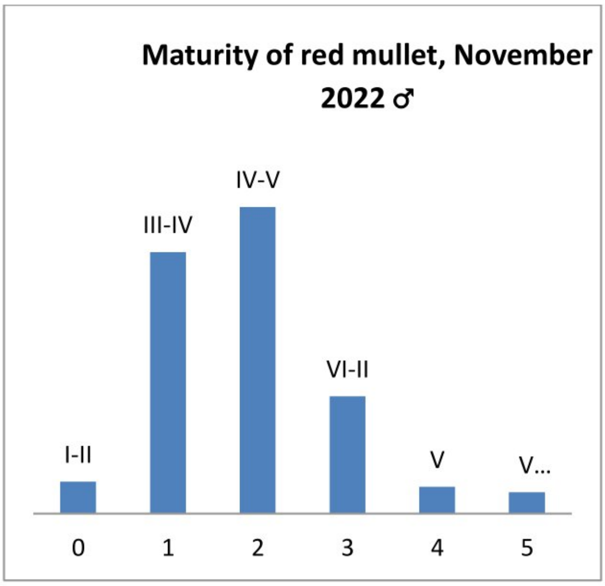


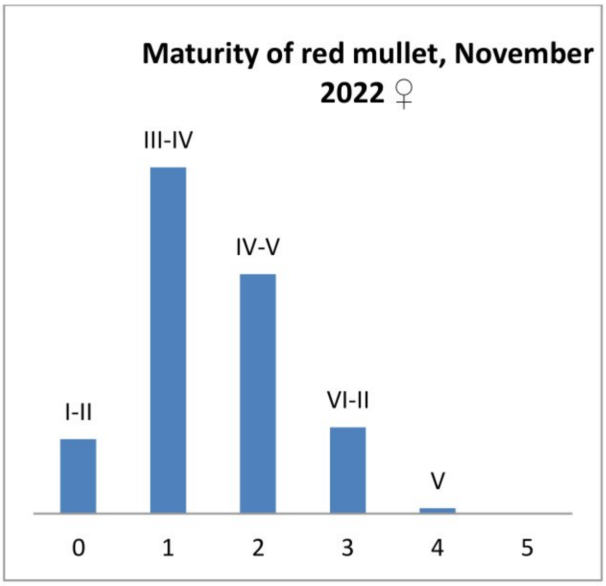


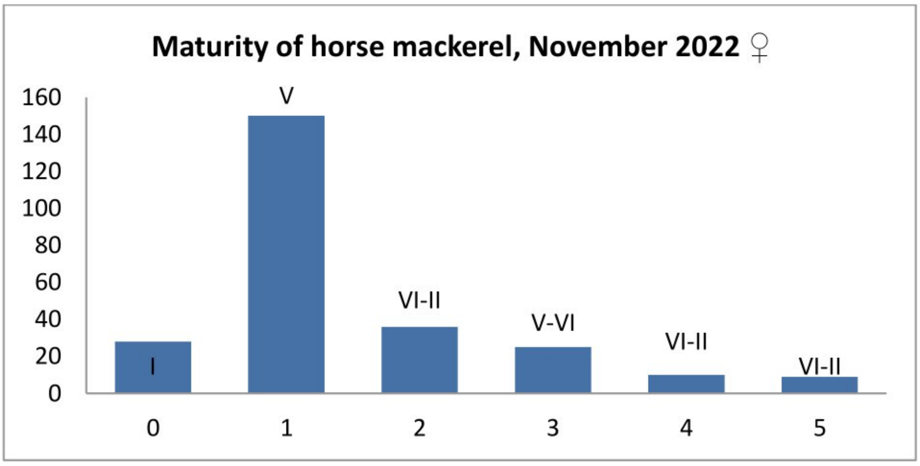


**Figure 12.3.** Sexual maturity (males and females) of the studied species analysed by age groups

### 12.1. Fecundity and Gonado-somatic index (GSI)

The gonado-somatic index GSI (%) of sprat (females) is indicative for portional spawning ($R^2$ = 0.98) (Fig. 13.1.1a). In red mullet (Fig.12.1.1b) and whiting (Fig.12.1.1c) there is a very strong relationship between the weight of the gonads and the gonadosomatic index ($R^2$ = 0.87), which is an indication of the processes of mass reproduction and active maturation of sexual products during the study period. In horse mackerel, the relationship between the weight of the gonads and GSI is relatively low (Fig.12.1.1d).

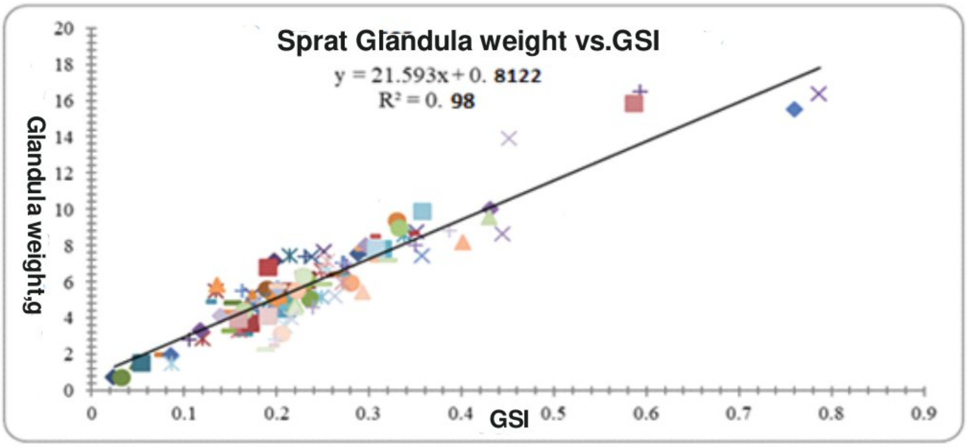


a)

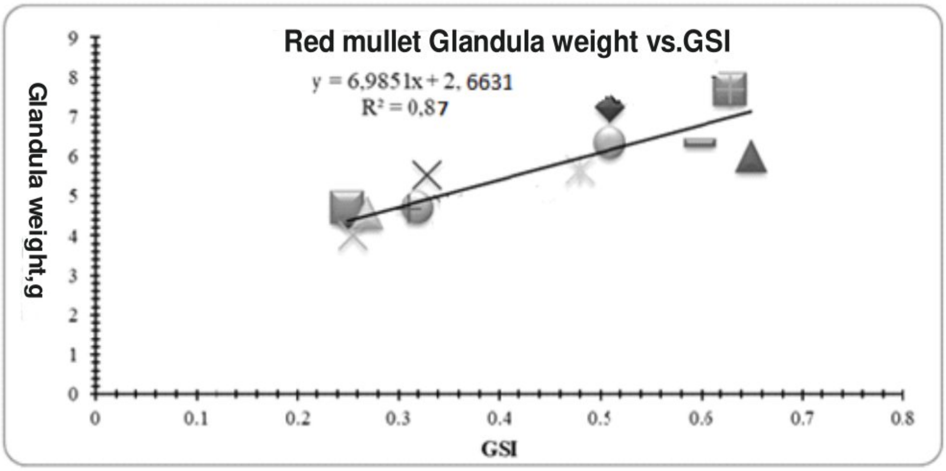


b)

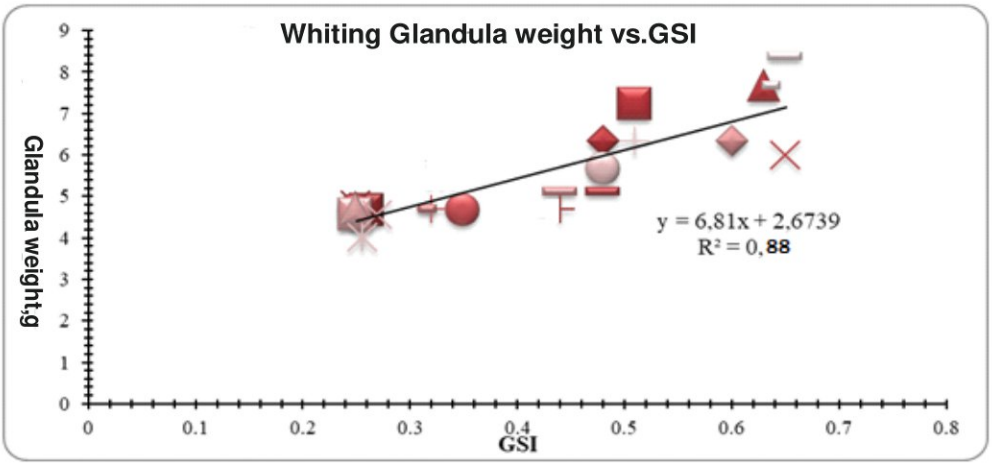


c)

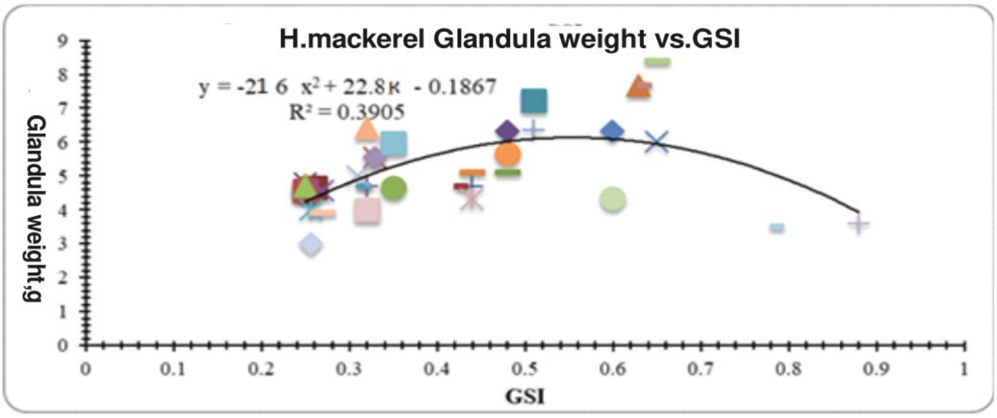


d)

**Figure 12.1.1.** Gonadosomatic index of a) sprat, b) red mullet, c) whiting, d) horse mackerel for the study period (GSI, %)

## 13. Natural mortality

Pauly's formula (Pauly, 1980) was used to determine natural mortality for sprat. The values calculated for the natural mortality of the species were calculated as follows: When applying the asymptotic length in the formula: M = 0.763. When applying the asymptotic weight in the formula: M = 0.582. In the present study, a value for the natural mortality of sprat of 0.95 was used (Ivanov and Beverton, 1985; Prodanov et al., 1997).

## 14. Feeding

**Length-Weight Relationship (LWR), index of stomach fulness (ISF)**

In the measured sprat specimens, the absolute length reached an average of 9.40 cm ± 1.07 (SD) and the average weight was 6.04 g ± 2.14 (SD). Accordingly, the mean horse mackerel length was 9.36 cm ± 0.9 (SD), with a mean weight of 6.57 g ± 2.05 (SD) (Table 14.1).

**Table 14.1.** Summary data of length (L, cm), weight (W, g), and ISF (% of BW) of planktivorous fish: sprat (1) and horse mackerel (2), determined by stomach content analysis in XI.2022.

1. Sprat

| | L, cm | W, g | ISF, % BW |
|---|---|---|---|
| Mean | 9.40 | 6.04 | 1.88 |
| Standard Error | 0.24 | 0.48 | 0.34 |
| Median | 9.25 | 5.90 | 1.45 |
| Mode | 9.50 | 6.60 | #N/A |
| Standard Deviation | 1.07 | 2.14 | 1.52 |
| Sample Variance | 1.15 | 4.56 | 2.31 |
| Kurtosis | 0.45 | -0.08 | -1.23 |
| Skewness | 0.72 | 0.44 | 0.55 |
| Minimum | 7.80 | 2.50 | 0.18 |
| Maximum | 12.00 | 10.30 | 4.70 |
| Sum | 188.00 | 120.70 | 37.58 |
| Confidence Level (95.0%) | 0.50 | 1.00 | 0.71 |

2. Horse mackerel

| | L, cm | W, g | ISF, % BW |
|---|---|---|---|
| Mean | 9.36 | 6.57 | 0.66 |
| Standard Error | 0.14 | 0.32 | 0.09 |
| Median | 9.00 | 6.10 | 0.49 |

| | | | |
|---|---|---|---|
| Mode | 9.00 | 6.60 | #N/A |
| Standard Deviation | 0.90 | 2.05 | 0.59 |
| Sample Variance | 0.81 | 4.21 | 0.35 |
| Kurtosis | -0.21 | 0.68 | 8.74 |
| Skewness | 0.74 | 1.18 | 2.53 |
| Minimum | 7.90 | 3.70 | 0.03 |
| Maximum | 11.50 | 12.30 | 3.26 |
| Sum | 374.30 | 262.90 | 26.44 |
| Confidence Level (95.0%) | 0.29 | 0.66 | 0.19 |

A high average value of the stomach fullness index was recorded for the sprat - 1.88 % BW ± 1.52 (SD), while for the horse mackerel, this value was 0.66 % ± 0.59 (SD) (Fig. 14.1).

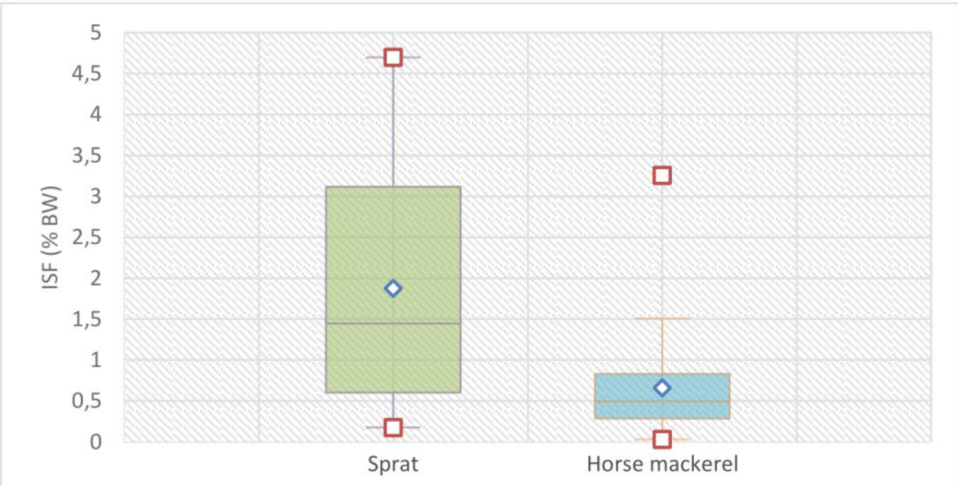


**Figure 14.1.** Box plot: ISF values (% BW) by species in XI. 2022 (indicated: medians, range of values: 25 – 75 %, minimum and maximum values)

It should be noted that the multiannual average value of autumn ISF for the sprat was 0.91 % BW, while for horse mackerel, the average ISF was 0.55 % BW ± 0.36 (SD) in the fall of 2020 and 0.35 % BW ± 0.27 (SD) in the fall of 2021. Accordingly, a more intensive feeding of sprat and horse mackerel was found during the current survey than in previous years.

**Prey number (PN), species composition of food and relative importance index (IRI) of zooplankton**

The average prey number in the sprat food was 207 ind/stomach ± 46.06 SE, and the maximum number of food organisms was 792 ind/stomach (Fig. 14.2) was associated with a high consumption of the copepods C*alanus euxinus* and *Pseudocalanus elongatus*.

In the horse mackerel diet, the average prey number is 229 ind/stomach ± 56.75 SE, with a maximum number of food organisms of 1627 ind/stomach, by a high consumption of the copepods *Acartia clausi* and *Paracalanus parvus*.

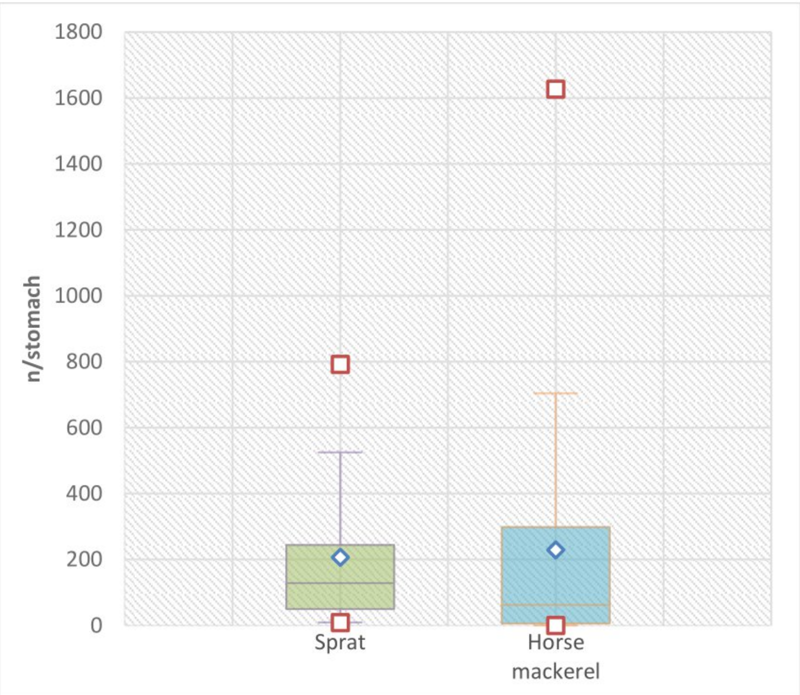


**Figure 14.2.** Box plot: Prey number (PN, ind/stomach) in the stomach content of the studied specimens by species in XI. 2022 (indicated: medians, range of values: 25 - 75 %, minimum and maximum values)

A small number of parasitic worm larvae were found in both the species (Fig. 14.3) and between 2.5 % (horse mackerel) and 5 % (sprat) of the examined fish were nematode larval carriers.

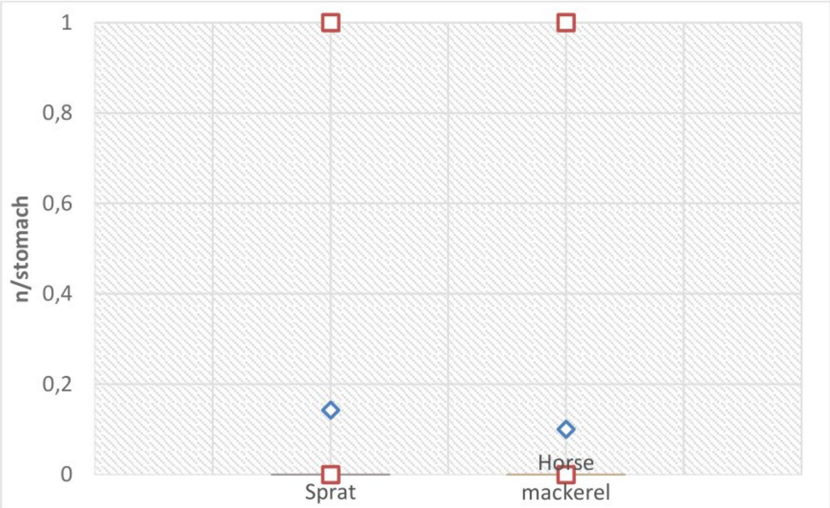


**Figure 14.3.** Box plot: Presence of parasitic organisms (n/stomach) in the stomachs of the studied specimens by species in XI. 2022 (indicated: medians, range of values: 25 - 75 %, minimum and maximum values)

In the zooplankton samples from the marine environment, 23 species/groups were identified, and only a part of them, seven species/groups, were present as components in the food of the sprat and 15 species/groups in the horse mackerel food.

The following groups and species are represented in the sprat diet: *Copepoda* ("oar-feet" crustaceans) - *Calanus euxinus*, *Pseudocalanus elongatus, Paracalanus parvus, Acartia clausi, and Oithona davisae;* from the planktonic larvae of bottom organisms (meroplankton), *Decapoda larvae are found;* class *Appendicularia* is represented by the species *Oicopleura dioica,* and phylum *Chaetognatha* by *Parasagitta setosa.* Accordingly, horse mackerel food consists of the following groups and species: Copepoda, *Pseudocalanus elongatus, Calanus euxinus, Paracalanus parvus, Acartia clausi*, *Oithona davisae, Centropages ponticus*; meroplankton - *Lamellibranchia veliger, Gastropoda veliger, Cirripedia larvae, and Decapoda*



*Project № BG14MFOP001-3.003-0004 Collection, management and use of data for the purpose of scientific analysis and implementation of the Common Fisheries Policy for the period 2022, funded by the Maritime and Fisheries Program and co-financed by the European Union through the European Maritime and Fisheries Fund*

*larvae,* phylum Chaetognatha - from *Parasagitta setosa*, class *Appendicularia, Oikopleura dioica.*

The indices of relative importance of the main zooplankton representatives in the food of the studied pelagic fish species, their percentage by number and biomass, and the frequency of occurrence are presented in Table. 14.2.

**Table 14.2.** The composition of pelagic fish species (XI. 2022)

1. Sprat

| Food composition | *N (%, of the total number)* | *M (%, of total biomass)* | *FO - Frequency of Occurrence* | *IRI - Relative Importance Index* |
|---|---|---|---|---|
| ***Calanus euxinus*** | 69.73 | 76.31 | 100 | 14603.8 |
| ***Pseudocalanus elongatus*** | 21.30 | 1.58 | 90 | 2059.3 |
| ***Paracalanus parvus*** | 1.00 | 0.03 | 30 | 30.8 |
| ***Acartia clausi*** | 0.83 | 0.09 | 35 | 31.9 |
| ***Decapoda larvae*** | 0.01 | 0.01 | 5 | 0.1 |
| ***Parasagitta setosa*** | 6.80 | 21.98 | 55 | 1583.3 |
| ***Oikopleura dioica*** | 0.31 | 0.01 | 15 | 4.8 |
| **Others** | 0.01 | 0.01 | | |
| **Total** | 100.00 | 100.00 | | 14603.8 |

2. Horse mackerel

| Food composition | *N (%, of the total number)* | *M (%, of total biomass)* | *FO - Frequency of Occurrence* | *IRI - Relative Importance Index* |
|---|---|---|---|---|

| | | | | |
|---|---|---|---|---|
| ***Calanus euxinus*** | 6.43 | 27.30 | 27.50 | 927.6 |
| ***Pseudocalanus elongatus*** | 6.22 | 4.98 | 62.50 | 700.5 |
| ***Paracalanus parvus*** | 59.21 | 25.05 | 77.50 | 6530.1 |
| ***Acartia clausi*** | 16.45 | 24.22 | 77.50 | 3151.9 |
| ***Centropages ponticus*** | 0.35 | 0.72 | 30.00 | 32.1 |
| ***Oithona davisae*** | 0.45 | 0.05 | 22.50 | 11.2 |
| ***Penilia avirostris*** | 2.37 | 3.91 | 40.00 | 251.1 |
| ***Cirripedia cypris, nauplii*** | 0.40 | 0.18 | 25.00 | 14.4 |
| ***Decapoda larvae*** | 0.33 | 1.94 | 20.00 | 45.4 |
| ***Parasagitta setosa*** | 0.20 | 9.92 | 15.00 | 151.8 |
| ***Oikopleura dioica*** | 6.11 | 1.46 | 37.50 | 283.8 |
| ***Pisces ova*** | 0.12 | 0.22 | 7.50 | 2.6 |
| ***Lamellibranchia veliger*** | 0.06 | 0.01 | 17.50 | 1.2 |
| **Others** | 1.30 | 0.04 | | |
| **Total** | 100.00 | 100.00 | | |

Among the samples studied, dominant role in the sprat food has *C. euxinus, Ps. elongatus and P. setosa* (Table 14.2, Fig. 14.4). The horse mackerel food is dominated by *P. parvus, A. clausi, Ps. elongatus* and *C. euxinus* (Table 14. 2, Fig. 14.4).



*Project № BG14MFOP001-3.003-0004 Collection, management and use of data for the purpose of scientific analysis and implementation of the Common Fisheries Policy for the period 2022, funded by the Maritime and Fisheries Program and co-financed by the European Union through the European Maritime and Fisheries Fund*

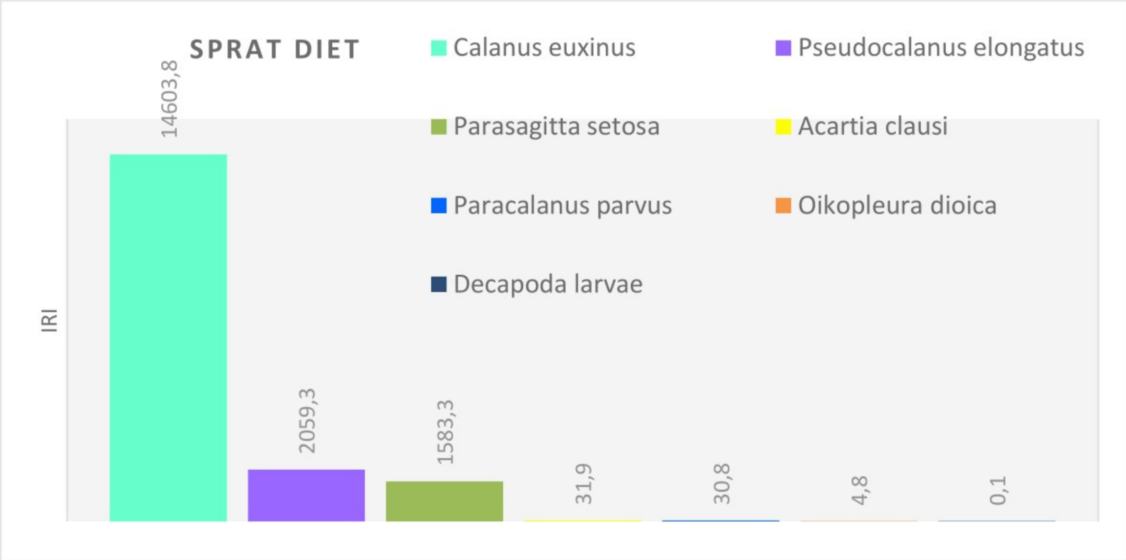


1.

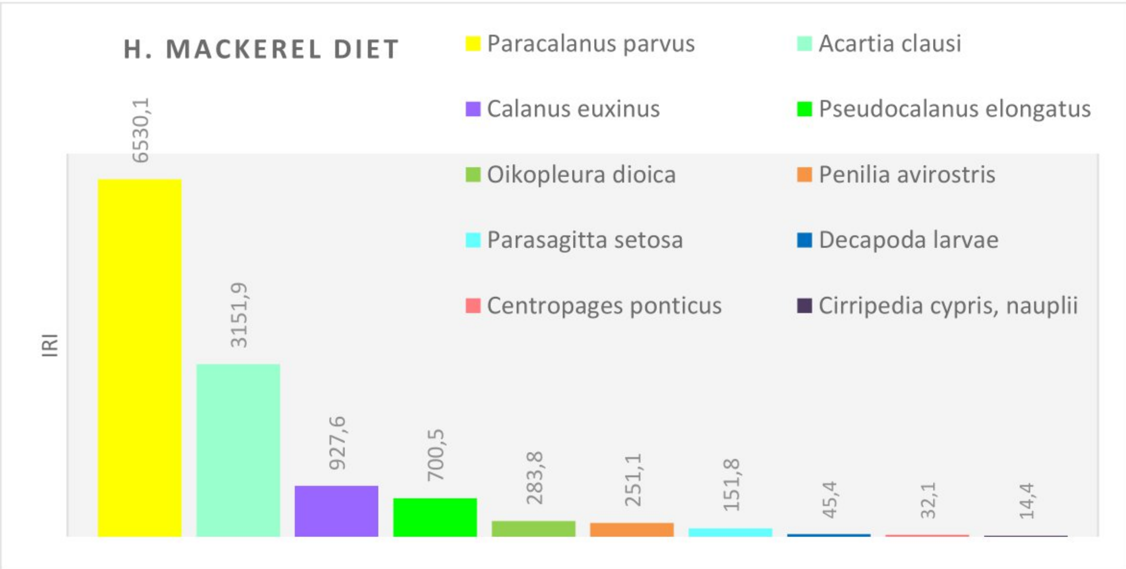


2.

**Figure 14.4.** Mean values of the relative importance indices (IRI) of the main mesozooplankton species in the food of sprat (1) and horse mackerel (2) during XI. 2022

## Species composition and quantity of zooplankton in the marine environment

During the study period, zooplankton biodiversity comprised 23 species and groups of organisms (Table 14.3).

**Table 14.3.** Species composition of zooplankton

| | XI. 2022 |
|---|---|
| 1. | Noctiluca scintillans |
| 2. | Aurelia autria |
| 3. | Calanus euxInus |
| 4. | Pseudocalanus elongatus |
| 5. | Paracalanus parvus |
| 6. | Oithona similis |
| 7. | Oithona davisae |
| 8. | Acartia clausi |
| 9. | Centropages ponticus |
| 10. | Cyclopoida spp. |
| 11. | Harpacticoida spp. |
| 12. | Pleopis polyphemoides |
| 13. | Penilia avirostris |
| 14. | Polychaeta larvae |
| 15. | Lamellibranchia veliger |
| 16. | Gastropoda veliger |
| 17. | Cirripedia larvae |
| 18. | Decapoda larvae |
| 19. | Phoronis larvae |
| 20. | Nematoda larvae |
| 21. | Parasagitta setosa |
| 22. | Oicopleura dioica |
| 23. | Pisces ova, larvae |



*Project № BG14MFOP001-3.003-0004 Collection, management and use of data for the purpose of scientific analysis and implementation of the Common Fisheries Policy for the period 2022, funded by the Maritime and Fisheries Program and co-financed by the European Union through the European Maritime and Fisheries Fund*

Protozoa (45.97%), Copepoda (31.40%), and Cladocera (13.87%) had a dominant role in the formation of the average mesozooplankton biomass (Fig. 14.5; Table 14.4), and jelly like zooplankton were only represented by *Aurelia* aurita (Fig. 14.5).

The dominant groups in terms of abundance were Copepoda (48.33%) and Protozoa (28.18%), followed by Cladocera (8.88% (Fig. 14.5).

1.
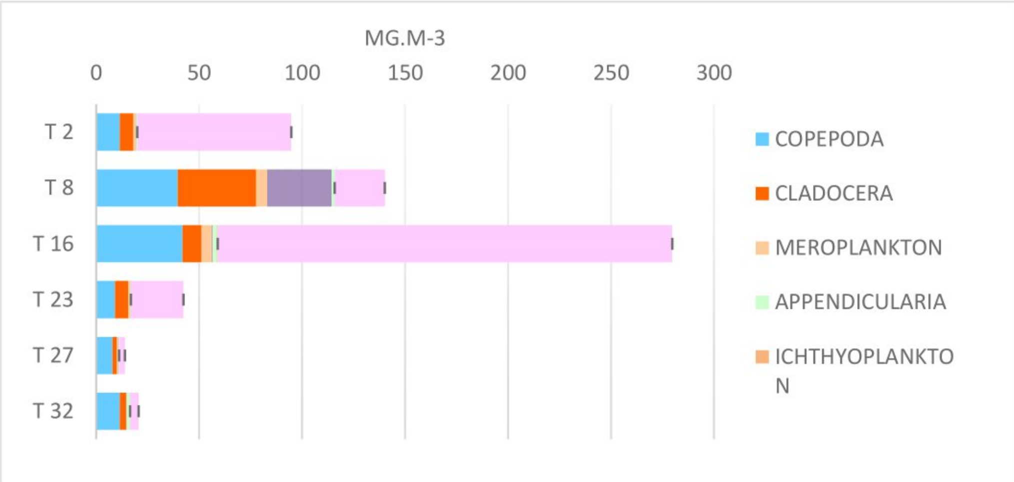


2.
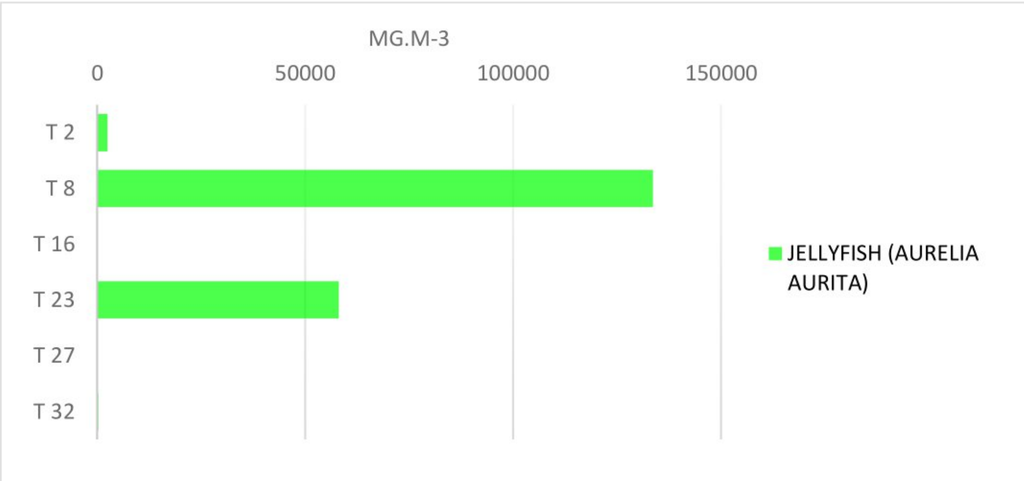

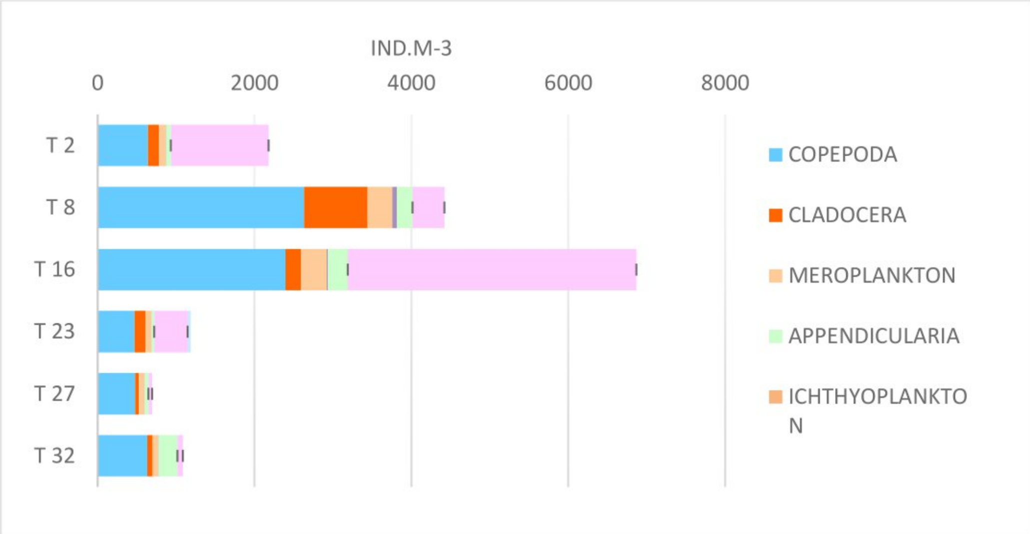


3.

**Figure 14.5.** Distribution of mesozooplankton biomass (1, mg.m $^{-3}$) and jelly like zooplankton (2, mg.m$^{-3}$), and abundance of the main zooplankton groups (3, ind.m $^{-3}$) by station in XI. 2022

**Table 14.4.** Percentage shares (% relative to biomass mg.m$^{-3}$) of the main zooplankton groups by station in XI. 2022

| *station* | *Copepoda* | *Cladoera* | *Meroplankton* | *Chaetognatha* | *Appendicularia* | *Ichthyoplankton* | *NOCTILUCALES* |
|---|---|---|---|---|---|---|---|
| **T2** | 12.08 | 7.10 | 1.29 | 0.10 | 0.48 | 0.00 | 78.96 |
| **T8** | 28.25 | 27.20 | 3.80 | 22.25 | 1.12 | 0.00 | 17.38 |
| **T16** | 14.99 | 3.33 | 1.74 | 0.18 | 0.72 | 0.14 | 78.90 |
| **T23** | 21.33 | 15.51 | 2.38 | 0.03 | 0.49 | 0.00 | 60.27 |
| **T27** | 55.96 | 15.13 | 5.84 | 0.19 | 2.68 | 0.00 | 20.20 |
| **T32** | 55.78 | 14.95 | 1.54 | 0.12 | 7.51 | 0.00 | 20.10 |
| **total** | 31.40 | 13.87 | 2.76 | 3.81 | 2.17 | 0.02 | 45.97 |

Table 14.5 presents summarized statistical data regarding the total biomass of zooplankton and the main constituent subgroups: mesozooplankton, jelly like zooplankton, and protozoans. The

total biomass of zooplankton is high - 32.53 gm $^{-3}$ ± 22.32 (SE), due to significant biomass of jelly-like species - 32.43 gm $^{-3}$ ± 22.31 (SE). The biomass of food zooplankton was low for the season – 39.87 mg.m$^{-3}$.

**Table 14.5.** Summary data on the total biomass (mg.m$^{-3}$) of zooplankton and the main groups in XI. 2022

| | *Meso-zooplankton* | *Jelly-like zooplankton* | *Protozoa* | *Total zooplankton biomass* |
|---|---|---|---|---|
| Mean | 39.87 | 32428.37 | 58.74 | 32526.98 |
| Standard Error | 16.77 | 22315.67 | 34.10 | 22319.08 |
| Median | 18.39 | 1389.53 | 24.96 | 1447.21 |
| Standard Deviation | 41.07 | 54662.00 | 83.54 | 54670.35 |
| Kurtosis | 2.31 | 2.34 | 3.96 | 2.34 |
| Skewness | 1.68 | 1.70 | 1.98 | 1.70 |
| Minimum | 11.14 | 0.00 | 2.82 | 13.96 |
| Maximum | 115.80 | 133650.90 | 220.74 | 133791.06 |
| Sum | 239.21 | 194570.22 | 352.44 | 195161.87 |
| Confidence Level (95.0%) | 43.10 | 57364.26 | 87.67 | 57373.01 |

During the study, the mesozooplankton biomass was maximal, up to 115.79 mg.m$^{-3}$ in front of the northern coast (Fig. 14.6). *Protozoa* were concentrated at – 220.74 mg.m$^{-3}$ in front of Cape Emine (Fig. 14.6), while the main accumulation of jelly like zooplankton, 133.65 gm$^{-3}$, was observed in the front of the northern coast (Fig. 14.6).

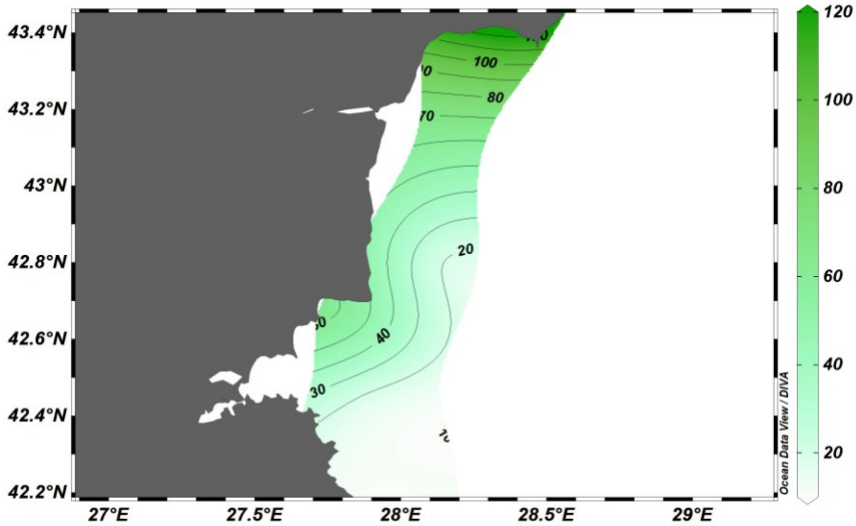
43.4°N
43.2°N
43°N
42.8°N
42.6°N
42.4°N
42.2°N
27°E
27.5°E
28°E
28.5°E
29°E
100
80
70
20
40
30
120
100
80
60
40
20
Ocean Data View / DIVA

1.

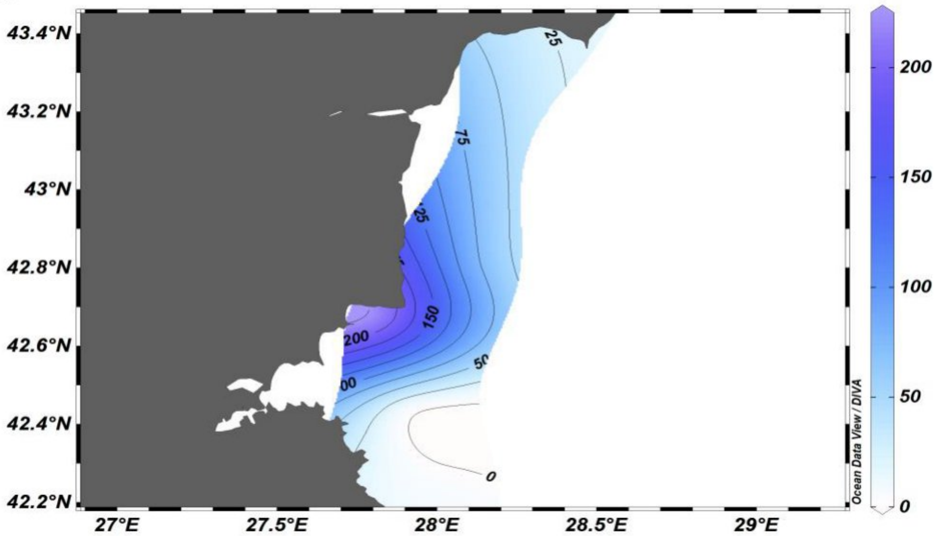
43.4°N
43.2°N
43°N
42.8°N
42.6°N
42.4°N
42.2°N
27°E
27.5°E
28°E
28.5°E
29°E
25
75
150
200
50
0
200
150
100
50
0
Ocean Data View / DIVA

2.

3.

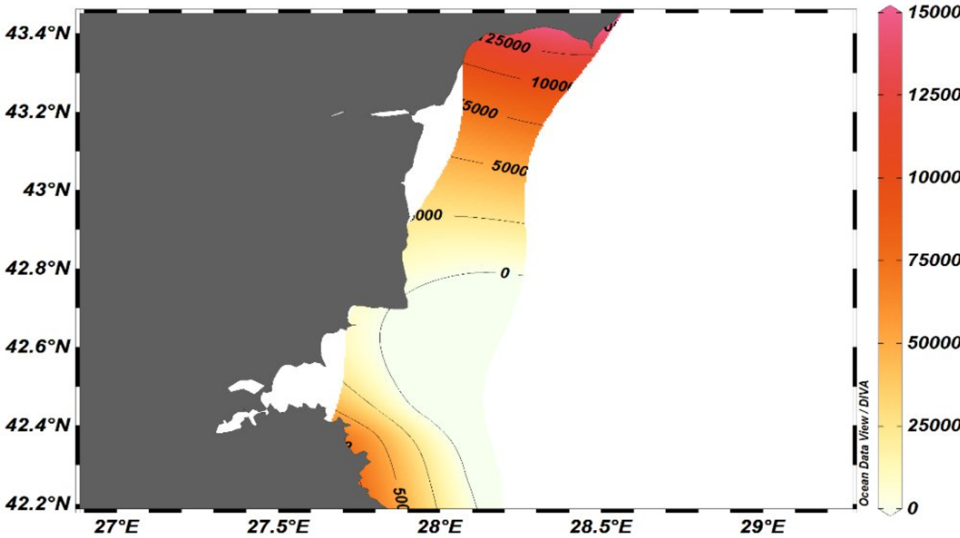


**Figure 14.6.** Spatial distribution of biomass (mg.m$^{-3}$): mesozooplankton (1), protozoa (2), and jelly like zooplankton (3) during XI. 2022

## 15. MSY – Maximum ssustainable yield

**Table 15.1.** Maximum sustainable yield (Sparre &Venema, 1992); 2/3 MSY ( FAO, 1995)

| Species | Biomass, t | MSY, t | 2/3MSY,t | TAC,t |
|---|---|---|---|---|
| **Red mullet** | 8854,217 | 4427,1085 | 2951,406 | 2900 |
| **Whiting** | 5576,516 | 2788,258 | 1858,839 | 1800 |
| **Horse mackerel** | 2203,66 | 1101,83 | 734,5533 | 700 |

The MSY, according to the precautionary approach (FAO, 1995) is calculated as 2/3 MSY for the selected species biomass. TAC -Total allowable catch recommended following the precautionary approach ( table 15.1.).

# 16. Conclusions

Feeding and diet composition

- In the autumn of 2022, **the food spectrum** of sprat included seven species/groups of zooplankton, and 15 species/groups were found in horse mackerel food. In the sprat diet were found Copepods ("oar-feet" crustaceans) - *Calanus euxinus, Pseudocalanus elongatus, Paracalanus parvus, Acartia clausi, and Oithona davisae,* from the group of planktonic larvae of bottom organisms (meroplankton) are found *Decapoda larvae*; class Appendicularia is represented by the species *Oicopleura dioica*, and phylum Chaetognatha - by *Parasagitta setosa*. Accordingly, the horse mackerel food consists of the following groups and species: Copepoda - *Pseudocalanus elongatus, Calanus euxinus, Paracalanus parvus, Acartia clausi, Oithona davisae*, *Centropages ponticus* ; meroplankton - *Lamellibranchia veliger* , *Gastropoda veliger, Cirripedia larvae* , and *Decapoda larvae* , type Chaetognatha - from *Parasagitta setosa* , class Appendicularia - *Oikopleura dioica*
- **The dominant species** in sprat food is ***C.*** *euxinus* (IRI = 14603.8), *Ps. elongatus* (IRI = 2059.3) *and P. setosa* (IRI = 1583.3). The horse mackerel food is dominated by *P. parvus* (IRI = 6530.1), *A. clausi* (IRI = 3151.9), *C. euxinus* (IRI = 927.6), and *Ps. elongatus* (IRI: 700.5).
- **A high mean ISF value** was recorded for sprat -1.88 % BW ± 1.52 (SD); while for the horse mackerel, this index was 0.66 % ± 0.59 (SD).
- **The average prey number** in the sprat food is 207 ind/stomach ± 46.06 SE, and the maximum number of food organisms - 792 ind/stomach was related to a high consumption of *copepods Calanus euxinus and Pseudocalanus elongatus*. In the horse mackerel diet, the average prey number was 229 ind/stomach ± 56.75 SE, and the maximum number of food organisms was 1627 ind/stomach, in relation to the consumption of the copepods *Acartia clausi* and *Paracalanus parvus*.
- **The total zooplankton biomass in the marine environment** was high - 32.53 $g.m^{-3}$ ± 22.32 (SE), but 99.7% of this value was formed by jelly like species, 0.18% by Protozoa, and 0.12% by fodder mesozooplankton. The average mesozooplankton biomass was 39.87 $mg.m^{-3}$, with maximum values of 115.80 $mg.m^{-3}$ in front of the northern part of the Bulgarian coast.

**Sprat** *(Sprattus sprattus)*



*Project № BG14MFOP001-3.003-0004 Collection, management and use of data for the purpose of scientific analysis and implementation of the Common Fisheries Policy for the period 2022, funded by the Maritime and Fisheries Program and co-financed by the European Union through the European Maritime and Fisheries Fund*

The species was very poorly represented (only in a few control trawls), with 59 specimens. The almost complete absence of the species speaks of its scattered behavior in front of the Bulgarian coast in November 2022. The low number of trizona individuals caught in November 2022 (n=59) did not allow calculation of asymptotic length and growth parameters. The predominant age group in the sprat (n = 59) during the study period was 1-1+ (46.6%), followed by 2-2+ (33%). The length-weight relationship in the trizone is described with the model W = 0.00575.L3,23, showing positive allometric growth ( ≥ 3 ), the resulting nonlinear LWR model displayed very high statistical validity (R2 = 0.9973). Recruitment was represented with 2,55% share of total catches. Sex ratio бе 49:48 (females vs males individuals) and 3 % share of juveniles forms. The 2+ year olds with maturity level IV-V had the largest share.

**Red mullet** *(Mullus barbatus)*

- The densest agglomerations of the red mullet were recorded at depths of 30-50 m with an average catch per unit area CPUA = 4432,442 kg.km$^{-2}$ (depth ~ 30-40 m) in front of Primorsko and Sozopol, Dolni Chiflik and Nessebar, followed by catch per unit area at depth 50-100 m (CPUA = 148,335 kg.km$^{-2}$). In the survey conducted in November 2022 in the depth layer 15-30 CPUA of red mullet was relatively low – 95 kg.km$^{-2}$;

- In November 2022, the red mullet biomass in the 30-50 m layers was estimated at 8044.085 tons, followed by the 50-100 m layers - 408.471 tons and 15-30m - 197.43 tons and (precisely in these depths in November 2022). The studied area was 8010,24 km$^{-2}$, and the total biomass was assessed to 8 854,217 t;

- The CPUA kg.km$^{-2}$ was significantly higher in the 30-50m layers, with the formation of mullet agglomerations. The densest agglomerations are observed in front of (southern) Sozopol and Primorsko; in front of Dolni Chiflik (2 stations) and in Nessebar Bay (1 station);
- The LWR is described best with the model W = 0.00575.L3,23, showing positive allometric growth ( ≥ 3 ), the resulting nonlinear LWR model displayed very high statistical validity ($R^2$ = 0.9973);
- During the study, the smallest size class was 6 cm and the largest was 16.5 cm, with predominant size classes in the catch composition 11-12 cm. The other size classes were less represented;
- The length-weight dependence in mullet is strong, showing positive allometry with a high coefficient of determination $R^2$ = 0.9973;
- During the study, the predominant size classes in the composition of the catch were 11.0-11.5 - 12 cm;

- The distribution of age groups in the red mullet was similar to that of the whiting, the recruitment was represented by a smaller share (~ 0%). The age structure of the red mullet was represented by 5 groups, with the predominant class being 2-2+ $y^{-1}$;

- The sex structure of the red mullet was in the ratio of 49:51 (male: female). The 1+ and 2+ year olds with degrees of maturity 1+(III-IV), 2-2+(IV-V) had a predominance.

**Whiting** *(Merlangius merlangus)*

- The highest average value of the mejid biomass was observed in the 15-30 m layer: 2935.731 t. In the remaining two depth layers 30-50 m and 50-100 m the values are 1985.366 and 655.4191t. The spatial distribution of the whiting was scattered, with higher clusters being established in the 30-50m stratum, opposite Obzor, Banya village, Arkutino/ Primorsko and south of Sozopol;
- The studied area was 8010.24 $km^{-2}$, and the total biomass was estimated to - 5576,516 t.;
- In the depth layer 30-50 m were registered the highest CPUA - 8727,75 $kg.km^{-2}$, with average quantities of 1093,974 $kg.km^{-2}$. In depth layer 15-30 m, 3173,727 $kg.km^{-2}$ and average CPUA 1421,565 kg.km-2; 50-100 m – 581,85 $kg.km^{-2}$ and average CPUA 158,6864 $kg.km^{-2}$, the species was registered in all control trawls;
- The LWR of the whiting was described by the model $W= 0.0711.L^{2.19}$, with positive allometric growth $\leq 3$, the resulting nonlinear LWR model displayed very high statistical validity ($R^2 = 0.943$);
- The length distribution of whiting LFD samples was bimodal, with peaks at 11.5-12.5 and 14-14.5 cm. A peak was observed in the 14 cm size group;
- The age structure of whiting was ranging from 0 to 5+ years, with the most significant representation of the 4+ age group;
- Whiting and horse mackerel are characterized by lower growth rates but a relatively high asymptotic length value, similar to the red mullet, with the exception of horse mackerel due to the small number of individuals caught and studied;
- The highest numbers of presentation in the whiting catches had size classes 11.5–12.5 and a maximum at 14 cm;
- The most abundant age groups of whiting were 1 and 4 years old, with age groups 0+ and 5 characterized by low abundance indices in November 2022;
- The sex ratio was 49:49 with 2% juvenile forms (immature);

- Maturity level – with the highest percentage of stage III-IV, were 1-1+ year old females; among males, there was a preponderance of 2-2+ year olds with grade IV-V;
- Whiting has a very strong correlation between the weight of the glands and the gonadosomatic index ($R^2 = 0.87$), which is an indication of mass reproduction processes and active maturation of sexual products during the studied period.

**Horse mackerel** *(Trachurus mediterraneus)*

- The horse mackerel is a migratory species in front of the Bulgarian coast of the Black sea. In November 2022, the species formed dense aggregations in the deep layers;
- The highest average biomass values were recorded in the 30-50m layer (1059,066 tons, east of Primorsko), followed by 1006,503 tons in the 50-100m layer. At depths of 15-30m, we observed the smallest aggregations of horse mackerel - 138.09 tons. The total instantaneous biomass in November 2022 was assessed to 2203.66 tons;
- At depths of 30-50m, in two of the studied stations, peaks in catch per unit area of 5243.408 and 5039,589 $kg.km^{-2}$ were observed in front of Primorsko;
- In the rest of the stations, the variation of the catch per unit area was in a wide range from 17 to 628 $kg.km^{-2}$. Mean values by stratum were as follows: 15-30 m: 66,87 $kg.km^{-2}$; 30-50 m: 584 $kg.km^{-2}$; 50-100m: 244 $kg.km^{-2}$;
- The LWR of the horse mackerel was described by the model $W = 0.0029.L^{3,35}$, the allometric growth was positive $\geq 3$, the resulting nonlinear LWR model displayed very high statistical validity ($R^2 = 0.99$);
- The length distribution in the horse mackerel samples was bimodal, with peaks at 12.5 and 14 cm;
- In horse mackerel, the age group 2-2+ $y^{-1}$ prevailed over other age groups. The share of age groups 1-1+ and 3-3+ is two times lesser than those of the two years old;
- In November 2022, the share of saffron with size classes 8.5, 9.5 and 12 -12.5 cm was the highest. The largest number was in the age group 1+ years and 0+ years;
- Horse mackerel biomass was relatively low for size classes 6.5 to 9, 15.5 cm, with the highest values being reached at 11.5-12.5, 14, 14.5 cm and age group 1-1+ and 4+ years;
- The female and male specimens of the sprat, whiting, horse mackerel and red mullet were represented in percentage as follows: 50:49%. Young specimens are represented by a very small percentage (1-3%);
- A predominance of females aged 1-1+ (V degree of maturity) was observed.

## 17. References

Bertalanffy L. VON 1938. A quantitative theory of organic growth (Inquiries on growth laws. II). Human Biol. 10: 181-213.

Gulland J.A., 1966. Manual of sampling and statistical methods for fisheries biology. Part I: Sampling methods. FAO Manuals in Fisheries Science No. 3, Rome.

Gulland J.A., 1970. The fish resources of the ocean. FAO Fish. Techn. Pap. No. 97, 1-425, Rome.

FAO: Precautionary approach to fisheries. FAO Fish. Tech. Paper N. 350 (1), 1995.

ICES. 2011. Report of the Workshop on Sexual Maturity Staging of Herring and Sprat (WKMSHS), 20-23 June 2011, Charlottenlund, Denmark. ICES CM 2011/ACOM:46. 143pp.

Kasapoglu, N., Duzgunes, E. 2014. Otolith Atlas for the Black Sea. Journal of Environmental Protection and Ecology 16, No 1, 133–144.

Kock,1985. Krill consumption by anthracitic notohenoid fish. In Antarctic Nutrient cycles and food webs. ED.W.R.Siegfried, P.R.Condy&R.M.Laws, pp.437.Berlin Springer Verlag

Korshenko, A., Alexandrov B., 2012. Manual for mesozooplankton sampling and analysis in the Black Sea monitoring (Black Sea Zooplankton Manual) Online: http://bsc.ath.cx/documents/ExpertNetwork/default.asp?I=/Expert%20Network%20-%20 Zooplankton.

Laevastu, T., 1965. Manual methods in fisheries biology. Observations on the chemical and physical environment. Chemical analysis of water FAO. Marine Physiological Sci., 6: 86-86.

Mordukhay-Boltovskoy, F.D. (Ed.). 1968. The identification book of the Black Sea and the Sea of Azov Fauna.- Kiev: Naukova Dumka Publ., T. 1 (Protozoa, Porifera, Coelenterata, Ctenophora, Nemertini, Nemathelminthes, Annelida, Tentaculata), 423 pp. (in Russian).

Pinkas L.,. Oliver M.S, Iverson I.L.K., 1971. Food habits of albacore, bluefin tuna and bonito in Californian waters. California Fish Game 152:1-105.

Pısıl, Y., 2006. Karadeniz'de Yaşayan Çaça Balığı (Sprattus sprattus (L., 1758))'nda Kemiksi Yapıları ve Uzunluk-Frekans Metodu ile Yaş Tayini. 19 Mayıs Üniversitesi, Fen Bilimleri Enstitüsü, Y. Lisans Tezi, 32 s.

Prodanov K., Mikhailov K., Daskalov G., Maxim C., Chashchin A., Arkhipov A., Shlyakhov V., Ozdamar E. 1997. Environmental management of fish resources in the Black Sea and their rational exploitation. Studies and Reviews. GFCM. No. 68. FAO, Rome.

Raykov V., Schlyakhov Vl., Maximov V., Radu Gh., Staicu I., Panayotova M., Yankova M., Bikarska I., 2008 - Limit and target reference points for rational exploitation of the turbot (Psetta maxima L.) and whiting (Merlangius merlangus euxinus Nordm.) in the western part of the Black Sea.VI Anniversary Conferense of the Institute of zoology. Acta Zoologica Bulgarica, 2008, Suppl.2: 305-316, ISSN 0324- 0770.

Raykov V, Yankova M, Radu Gh., Lisichkov K., 2009 - Exploitation patterns call for limit the sprat catches off the north-western coast of the Black sea.Intern.Conf.:Sustainability in South-eastern Europe"Tekirdag, Istanbul 16-20 VI.(under review for JEPE).

Raykov V., I. Staicu, G. Radu, V. Maximov, S. Nicolaev, 2008 – Specificity of the fishery and common fishery policy implementation: a case study of the western part of the Black Sea. Cercetari marine. Recherches marines. INCDM. 38: 223-232, ISSN:0250-3069, Cod CNCSIS: 74.

Raykov,V. M Yankova., V. Mihneva,.Dineva S., Petrova D. M. Panayotova, 2008 Stock Assessment of Sprat (Sprattus sprattus) by Swept Area Method during the spring season of 2008 along the Bulgarian Black Sea coast. Technical report, 2008.

Raykov V.S, V.V.Mihneva, Daskalov, and G: Investigations on sprat (*Sprattus sprattus* L.) population dynamics related to its trophic base and climate change over the period 1996-2004 in Bulgarian waters of the Black Sea. J.Environmental Protection and Ecology, 8 (2) (2007), 319-332.

Raykov, V, Panayotova M, Stefanova K, E. Stefanova 2011.Stock assessment of sprat in Bulgarian marine area, Institute of Fish resources and National Agency for fisheries and Aquaculture – Bulgaria in accordance with the Council Regulation (EC) № 199/2008 establishing a community framework for the collection, management and use of data in the fisheries sector and support for scientific advice regarding the common fisheries policy. 100 pp.

Simon, K.D., Y. Bakar, A.G. Mazlan, C.C. Zaidi and A. Samat et al., 2012. Aspects of the reproductive biology of two archer fishes Toxotes chatareus, (Hamilton, 1822) and Toxotes jaculatrix (Pallas, 1767). Environ. Biol. Fish., 93: 491-503.

Sparre, P., & Venema, S. G. (1992). Introduction to tropical fish stock assessment part 1. manual FAO FISH. *Tech. Pap*, *306*(1).